Flavonols improve thermotolerance in tomato pollen during germination and tube elongation by maintaining ROS homeostasis

Anthony E. Postiglione[1], Allison M. Delange[1], Mohammad Foteh Ali[1], Maarten Houben[1], Eric Y. Wang[1], Stacy L. Hahn[1], Colleen M. Roark[1], Molly Davis[2], Robert W. Reid[2], James B. Pease[1], Ann E. Loraine[2], and Gloria K. Muday[1]

[1]Wake Forest University, Department of Biology and Center for Molecular Signaling, Winston Salem, NC

[2]University of North Carolina, Department of Bioinformatics and Genomics, Charlotte, NC

Running Heading: Flavonols protect tomato pollen from heat stress

Corresponding Author: Gloria K. Muday (muday@wfu.edu)

Author Contributions: AEP, AMD, EYW, MH, and GKM designed experiments. AEP, AMD, MFA, SLH, CMR, MH, and EYW performed research and analyzed data. MD, RWR, AEL, JBP performed computational analysis and/or wrote sections explaining the RNA-Sequencing data. AEP, AMD, and GKM wrote and edited the paper and all authors provided editorial suggestions.

Key words: tomato, pollen, flavonols, reactive oxygen species, heat stress, heat shock proteins

One sentence summary: Flavonol antioxidants reduce the negative impacts of elevated temperatures on pollen performance by reducing levels of heat induced reactive oxygen species synthesis and modulation of heat induced changes in the pollen transcriptome.

The author responsible for distribution of materials integral to the findings presented in this article in accordance with the policy described in the Instructions for Authors (https://academic-oup-com.wake.idm.oclc.org/plcell/pages/General-Instructions) is:
Gloria K. Muday (muday@wfu.edu)

ABSTRACT

Elevated temperatures impair pollen performance and reproductive success, resulting in lower crop yields. The *Solanum lycopersicum anthocyanin reduced* (*are*) mutant has a defect in the *FLAVANONE 3 HYDROXYLASE* (*F3H*) gene and impaired synthesis of flavonol antioxidants. We identified multiple aspects of pollen performance in *are* that were hypersensitive to elevated temperatures relative to the VF36 parental line, including heat-increased accumulation of reactive oxygen species (ROS). Transformation of *are* with an *F3H* transgene, or chemical complementation with flavonols, prevented temperature-dependent ROS accumulation in pollen and restored pollen performance to VF36 levels. Transformation of this *F3H* construct into VF36 (VF36-*F3H*-T3) prevented both temperature driven ROS increases and impaired pollen performance. RNA-Seq was performed at optimal and stress temperatures in *are*, VF36, and VF36-*F3H*-T3 at multiple timepoints across pollen tube emergence and elongation. All genotypes had increasing numbers of differentially expressed genes with duration of elevated temperature, with the largest number in *are* at all time points. These analyses also identified upregulated transcripts in *are*, relative to VF36, even at optimal temperatures, revealing a flavonol-regulated transcriptome. These findings suggest potential agricultural interventions to combat the negative effects of heat-induced ROS in pollen that leads to reproductive failure and crop loss.

INTRODUCTION

Global climate change has the potential to profoundly impact agriculture with increasing frequency of droughts, floods, and elevated temperatures. Global average temperatures are predicted to rise by as much as 3°C by the end of this century (Raftery et al., 2017), which is sufficient to negatively impact the yield of numerous crop species. Temperature-induced reductions in crop yields of rice, wheat, corn, and tomatoes have been shown to be as high as 30-50% (Sato et al., 2006; Fahad et al., 2017). Plant sexual reproduction is considered to be one of the weakest links in terms of susceptibility to increased temperature (Lohani et al., 2019). Elevated temperature can impair formation of viable pollen grains in the anthers, germination of mature pollen grains, pollen tube elongation, and fertilization of the ovules (Paupière et al., 2014; Rieu et al., 2017; Begcy et al., 2019; Raja et al., 2019; Chaturvedi et al., 2021). In tomato, heat stress impairs the development and function of pollen, with temperature-dependent effects observed at every step in this crucial process (Pressman et al., 2002; Firon et al., 2006; Sato et al., 2006; Lohani et al., 2019; Wu et al., 2020; Rutley et al., 2021). Therefore, it is imperative understand the molecular and cellular mechanisms by which elevated temperatures deleteriously affect pollen growth and development so that innovative strategies can be developed to prevent reproductive failure.

A major plant response to heat stress in reproductive tissues is increased accumulation of reactive oxygen species (ROS) (De Storme and Geelen, 2014; Muhlemann et al., 2018; Jahan et al., 2019; Torun, 2019), which may play a critical role in the observed reproductive impairments. ROS signaling is also necessary for both productive pollen tube germination and elongation, as well as coordinated tube lysis at the site of fertilization (Potocký et al., 2007; Speranza et al., 2012; Kaya et al., 2014; Jimenez-Quesada et al., 2019). However, unchecked ROS accumulation due to abiotic stresses, such as heat, can yield deleterious cellular effects including irreversible oxidative damage to nucleic acids, lipids, and proteins. Thus, oxidative stress has the ability to impact cellular processes and potentially lead to cell death (Møller et al., 2007). Although the mechanisms for synthesis of heat-dependent ROS and its biochemical targets have yet to be fully defined, the damaging effects that oxidative stress has on pollen performance are clear.

Plants employ various antioxidant mechanisms to maintain ROS homeostasis. This allows for localized ROS increases for signaling, while preventing ROS accumulation from reaching damaging levels (Chapman et al., 2019; Martin et al., 2022). These include the synthesis of enzymes that detoxify ROS such as superoxide dismutases (SODs), as well as small molecules, such as glutathione, that function as cellular antioxidants (Considine and Foyer, 2021). Plants also synthesize several classes of specialized metabolites that contain antioxidant capacity including carotenoids, tocochromanols, and flavonoids (Chapman et al., 2019; Daryanavard et al., 2023). The flavonoid class of metabolites include flavones, flavanone, flavonols and anthocyanins, with flavonols and anthocyanins having the highest radical scavenging abilities (Chapman et al., 2019; Daryanavard et al., 2023). Flavonols are found in many species, and plants with mutations that alter flavonol synthesis have been shown to have impaired reproductive success in rice, corn, petunia, and tomato (Mo et al., 1992; Pollak et al., 1993; Schijlen et al., 2007; Wang et al., 2020).

Flavonol biosynthesis is conserved across the plant kingdom, although the presence, or absence, of specific metabolic sequences leads to variation in which flavonoids accumulate in different species as well as in different tissues. For example, the flavonol myricetin is synthesized in *Solanum lycopersicum* (tomato), and many other species, but is not synthesized in Arabidopsis due to the absence of the gene encoding the branchpoint enzyme that produces this flavonol (Gayomba et al., 2017). Figure 1 illustrates the flavonol biosynthesis pathway in tomatoes, highlighting the metabolic sequence for synthesizing the three most abundant flavonols: kaempferol, quercetin, and myricetin. Additional modifications of flavonol backbones include methylation, as seen when O-methyl transferase 1 (OMT1) methylates quercetin to produce isorhamnetin, and addition of glycosyl groups to many flavonols, which produces a diverse array of distinct flavonols (Alseekh et al., 2020; Ku et al., 2020). Flavonols and anthocyanins differentially localize to distinct organs during various stages of development in tomatoes and other plants due to transcriptional regulation of pathway enzymes (Schijlen et al., 2007; Agati et al., 2012; Falcone Ferreyra et al., 2012; Pourcel et al., 2012; Groenenboom et al., 2013; Kovinich et al., 2014; Maloney et al., 2014; Gonzali and Perata, 2020). For instance, anthocyanins are not synthesized in tomato pollen and roots, due to the absence of expression of genes encoding enzymes that are late in the biosynthetic pathway that lead to anthocyanin synthesis (Maloney et al., 2014; Muhlemann et al., 2018).

An important role of flavonols in pollen has also been demonstrated in tomato (Schijlen et al., 2007; Muhlemann et al., 2018; Rutley et al., 2021). Silencing the expression of the *Chalcone Synthase* (*CHS*) gene, which encodes of the first enzyme of the flavonol biosynthetic pathway (see Figure 1), resulted in parthenocarpic (or seedless) fruits (Schijlen et al., 2007). The *are* mutant has a recessive point mutation in the single gene encoding *Flavanone 3-Hydroxylase* (*F3H)* gene. This mutation causes a loss of F3H activity (Yoder et al., 1994; Maloney et al., 2014) and has been shown to have reduced levels of flavonols in roots and leaves using Liquid Chromatography-Mass Spectroscopy (LC-MS) (Maloney et al., 2014). This mutant also contained reduced levels of flavonols in pollen (Muhlemann et al., 2018). The *are* mutant has significantly reduced pollen viability and pollen tube elongation at optimal temperatures compared to its parental line, which can be reversed by complementation with an *F3H* transgene (Muhlemann et al., 2018). Although that work reported impaired pollen tube elongation in the *are* mutant at elevated temperatures, there were many unanswered questions about the impacts of temperature on other aspects of pollen performance and whether these temperature effects were tied to flavonol levels.

This work explored the impact of elevated temperatures on multiple features of pollen performance in *are* and its wild-type parental background, VF36 and provided evidence for potential avenues of intervention. These analyses revealed the negative impact of elevated temperature on pollen yield, viability, germination, tube integrity, and tube elongation, with significantly more impact in *are* than its parental line. Additionally, both genetic and chemical complementation of *are* reversed the temperature hypersensitivity in *are* and overexpression of *F3H* conferred thermotolerance in pollen. Exogenous flavonols also protected pollen from temperature-impaired germination and tube elongation and prevented heat-dependent ROS accumulation, consistent with flavonols providing protection from temperature stress through their ROS scavenging capabilities. Additionally, the inhibition of enzymes that synthesize ROS reveal mechanisms that drive temperature stress induced ROS. Finally, we examined the transcriptional response to elevated temperature in wild-type, the *are* mutant, and the wild-type transgenic line engineered to over produce flavonols across a time course of control and temperature stress treatments, to reveal genes whose expression is heat-regulated, flavonol-regulated, and associated with impaired heat stress response. This work provides new insight into the mechanisms by which plants respond to heat stress which has the potential to translate to the

development of novel strategies to protect crops from elevated temperatures that result from our changing climate.

RESULTS

The *are* mutant has reduced pollen yield and viability and is hypersensitive to elevated temperatures

The effects of reduced flavonol synthesis on pollen yield were assessed using the *are* mutant, which contains a point mutation in the gene encoding flavanone 3-hydroxylase (F3H). The position of this enzyme in the flavonoid biosynthetic pathway is highlighted in Figure 1. To evaluate pollen yield in this mutant grown under standard greenhouse conditions, we harvested pollen from individual flowers. Pollen was resuspended in pollen viability solution (PVS) which allows pollen to hydrate without germinating, labeled with trypan blue, and quantified with a Countess II automated cell counter to determine the number of living grains in each flower. The quantification of pollen yield in both lines revealed that *are* had formed only 22% of the number of living pollen grains that were formed in VF36 (Figure 2A). These results are consistent with flavonol deficiency resulting in reduction of pollen yield.

To examine the effects of the *are* mutation on pollen viability at optimal and elevated temperatures, pollen samples were collected from plants grown under optimal conditions and incubated in PVS at 28°C (optimal temperature) or 34°C (heat stress) for 2 hours. At the end of this incubation, pollen grains were co-stained with 0.001% fluorescein diacetate (FDA) and 10 µM propidium iodide (PI) for 15 minutes to mark viable and non-viable grains, respectively (Figure 2B). Imaging with a laser scanning confocal microscope (LSCM) revealed that 70% of the VF36 grains were viable after exposure to optimal temperatures, while only 29% of *are* grains were viable (Figure 2C). When pollen from each genotype were exposed to temperature stress (34°C for 2 hours), these percentages fell to 51% for VF36, while only 3.5% of *are* pollen grains were viable. We also examined pollen viability in pollen directly after hydration in PVS using the same staining methods (Supplemental Figure 1). The percent viability of these pollen grains was similar to those hydrated for 2 hours, consistent with PVS incubation at optimal temperatures not affecting pollen viability over a 2-hour time course.

Genetic complementation of *are* with an *35S-F3H* transgene reversed pollen yield reduction and impaired viability and conveyed thermotolerance to VF36

We evaluated pollen yield in *are* and VF36 previously transformed with an 35S:*F3H* transgene (Maloney et al., 2014). The total yield of viable pollen in all three genotypes was quantified in individual flowers. The *are* transformant, *are 35S:F3H* Transgenic line 5 (abbreviated *are-F3H*-T5 or *are*-T5), produces 5 times more pollen than *are*, with a yield that is not significantly different than VF36. Flowers from VF36 *35S:F3H* Transgenic line 3 (VF36-*F3H*-T3 or VF36-T3) contained 2-fold greater yield of live pollen grains as compared to VF36 flowers and 9.1-fold greater yield than *are* (Figure 2A).

The viability of pollen at optimal and elevated temperatures was also examined in these transgenic lines. The *are F3H*-T5 line had significantly greater pollen viability than the *are* mutant, with pollen viability at levels equivalent to VF36 at both optimal and elevated temperatures (Figure 2B-C). The VF36 *F3H*-T3 transgenic line had similar percentages of viable pollen as VF36 at optimal temperatures, but when pollen was treated for 2 hours at 34°C the *VF36-F3H*-T3 line showed no reductions in pollen viability at this elevated temperature (Figure 2B-C), consistent with this transgene conferring thermotolerance.

To verify that both the *are* and VF36 lines transformed with the *35S-F3H* transgene had changes in pollen flavonol levels, we extracted flavonols from all four genotypes. Pollen from *are* contains 10-fold more of the F3H substrate, naringenin, than VF36 or the genotypes transformed with this construct (Supplemental Table 1). Pollen from *are* also had a significant reduction in the flavonol kaempferol, which is a metabolite downstream of the nonfunctional F3H enzyme in *are* (Figure 1). In the *are*-T5 line, both of these changes were reversed, resulting in levels of naringenin and kaempferol not being significantly different from VF36.

In *are*, pollen germination and tube elongation are hypersensitive to elevated temperatures and this effect is reversed by an *F3H* transgene

We asked whether impaired pollen germination under temperature stress was also accentuated in *are* and reversible by the 35S-*F3H* transgene. Pollen from all four genotypes was hydrated in pollen germination medium (PGM) for 30 min at either 28°C or 34°C and images were captured using an inverted light microscope. Representative images of pollen grains from,

are, VF36, *are*-T5 and VF36-T3 are shown in Figure 3A revealing a great number of ungerminated pollen grains and pollen grains or tubes that have burst. The percent germination is quantified in Figure 3B. There is only 61% germination of *are* pollen grains at optimal temperature relative to the other three genotypes that have ~80% germination. The impaired germination of *are* is accentuated at elevated temperature, where germination is reduced to 44%. In contrast, both the *are*-T5 and VF36-T3 lines have similar germination rates to VF36 at optimal temperature, but significantly greater germination than VF36 at elevated temperatures, suggesting that engineering plants to increase flavonol levels can enhance thermotolerance during pollen germination.

To verify that these effects were linked to the presence of the *F3H* transgene, we quantified germination in multiple separate *35S-F3H* transformants in the *are* and VF36 genotypes (Supplemental Figure 2). These transgenics line have similar ability to reverse the poor germination in *are* and convey thermotolerance to VF36. These findings are consistent with a model that the impaired pollen germination in *are* is linked to the *F3H* mutation and flavonols synthesized by a 35S promoter-driven *F3H* transgene is sufficient to complement the mutant temperature hypersensitivity phenotype. In both VF36-T3 and VF36-T5 lines we observed no reductions in germination at the higher temperature, consistent with these lines being resistant to the negative effect of elevated temperature on pollen germination (Figure 3B).

We also examined pollen tube elongation at optimal and elevated temperature in the *are* mutant, and asked whether impaired pollen tube elongation in *are* could be reversed with the *F3H* transgene. Pollen from the same four genotypes (VF36, *are*, *are*-T5, and VF36-T3) was hydrated in PGM before incubation at 28°C for 30 min to germinate pollen tubes. Half the samples from each genotype remained at 28°C for 90 min to allow pollen tube elongation and half were then transferred to 34°C for 90 minutes. Pollen tubes were then imaged via brightfield microscopy and tube length was measured.

At optimal temperatures, VF36 pollen tubes elongated 1.3-fold more than *are* pollen tubes after the 2-hour time course (Figure 3). Pollen tube length was significantly greater in *are-F3H*-T5 when compared to *are* with lengths not significantly different from VF36 (Figure 3D). We also observed that VF36-*F3H*-T3 pollen tubes were significantly longer than VF36 following

incubation at optimal temperatures, consistent with elevated flavonols protecting pollen tube growth from temperature stress.

Heat treatment significantly reduced pollen tube length in VF36 and *are*, relative to optimal temperature, with heat stressed *are* pollen having the shortest pollen tubes (Figure 3D). Tube extension at elevated temperatures was still decreased in the *are-F3H*-T5 line, though tube length was not significantly different than VF36 at this temperature. Additionally, pollen tube length in VF36-*F3H*-T3 was not significantly impaired by exposure to heat stress (Figure 3D). These data are consistent with the thermotolerance of pollen being dependent on the levels of flavonols, with reduced pollen tube length in *are* and VF36, while the *are*-T5 and the VF36-T3 transgenic lines displayed enhanced pollen tube elongation, especially under elevated temperature.

Pollen tube rupture is more prevalent in *are* at both temperatures and is not rescued via coincubation with VF36 pollen

We also evaluated the ability of flavonols to prevent pollen tube rupture. To assess this, we utilized a GFP construct driven by the pollen-specific promoter, *pLAT52*, that was transformed into the VF36 background (Zhang et al., 2008) and which we crossed into *are*. This allowed for pollen from VF36 *pLAT52:GFP* and *are* to be incubated together and tube rupture to be quantified for both samples simultaneously. Pollen tubes were elongated as described previously and the percentage of ruptured pollen tubes were quantified at both optimal and elevated temperatures. Incubation at 34°C significantly increased rates of pollen tube rupturing in both lines, though pollen tubes from VF36 *pLAT52:GFP* showed significantly lower rates of rupture when compared to *are* at both temperatures (Figure 4A-B). To verify that the discrepancy in pollen tube rupture seen between VF36 *pLAT52:GFP* and *are* was not due to the insertion of the transgene, we performed the reciprocal experiment (*are pLAT52:GFP*). Coincubation of *are pLAT52:GFP* with VF36 pollen once again showed higher rates of rupture in the *are* background regardless of temperature, suggesting that the presence of flavonols protects pollen tubes from bursting during elongation (Figure 4C). This data is also consistent with these constructs driving flavonol synthesis inside the pollen grain, as accumulation of flavonols on the outside of VF36 pollen grains/tubes have the potential to chemically complement the *are* pollen in close proximity and restore germination. However, since

coincubation of pollen from these two lines did not rescue impaired germination in *are* it appears that the flavonols are produced in the pollen interior.

ROS levels in pollen grains and tubes are inversely proportional to levels of flavonol antioxidants, and are increased at elevated temperature

To determine whether the protective effect of flavonols on pollen performance was due to their ROS scavenging activity in the pollen interior, we monitored ROS accumulation during the pollen germination and pollen tube elongation phases in VF36, *are*, *are-F3H*-T5, and VF36-*F3H*-T3 lines. We used 2'-7'-dichlorodihydrofluorescein diacetate (CM-H_2DCFDA, DCF), a chemical probe that can be oxidized by multiple ROS species, to quantify the relative levels of ROS accumulation in germinating pollen grains and elongating pollen tubes in these four genotypes under optimal and elevated temperatures.

ROS accumulation was examined during germination, pollen grains were hydrated in PGM at 28° or 34°C for 10 minutes and then further incubated in PGM containing CM-H_2DCFDA for an additional 20 minutes at the same temperatures to monitor ROS levels during the early stages of germination. The fluorescence intensity of pollen grains was then examined with a Zeiss 880 LSCM (Figure 5A), and these values are reported as a LUT, which makes the brighter fluorescence in *are* pollen easier to visualize. DCF fluorescence in mature, viable grains was then quantified and normalized to fluorescence intensity of VF36 at 28°C. At 28°C, pollen grains from the *are* mutant had a significant 1.4-fold higher DCF fluorescence than VF36 (Figure 5B). At 34°C, both genotypes exhibited significantly higher ROS levels relative to VF36 at 28°C. Heat stressed VF36 and *are* showed 1.4-fold and 1.7-fold higher fluorescence, respectively. The *are* transgenic line, *are-F3H*-T5, exhibited a significant 1.2-fold reduction in DCF relative to *are* at 28°C. *are*-T5 also had significantly reduced DCF fluorescence at 34°C relative to *are* at 34°C. The DCF fluorescence in pollen grains of the VF36-T3 line was not increased by elevated temperatures, with similar fluorescence at both 28°C and 34°C, consistent with enhanced thermotolerance and the absence of response to this acute heat stress (Figure 5B).

To evaluate ROS accumulation in elongating pollen tubes, pollen grains were allowed to germinate for 30 minutes at 28°C and then transferred to elevated temperature stress of 34°C for 90 minutes, while control samples remained at 28°C for the additional 90-minute period. Pollen tubes were then labeled with CM-H_2DCFDA for an additional 20 minutes and imaged as

described above (Figure 5C). This signal is bright throughout most of the tube, and the swollen tube tip in *are* at 34°C is consistent with a tube that is close to rupturing. It is also evident that the tube length of *are* is shorter, especially at elevated temperatures, while VF36-T3 tubes are longer than other genotypes, consistent with observations of pollen tube length in Figure 3C-D. DCF fluorescence was quantified in these pollen tubes revealing that heat stress significantly increased ROS accumulation in VF36 and *are* relative to VF36 at 28°C by 1.8- and 2.7-fold, respectively (Figure 5D). This substantially higher level of DCF signal in *are* at 34°C is consistent with elevated ROS leading to reduced pollen tube length at elevated temperature. These results indicate that increased flavonol synthesis maintains ROS homeostasis at elevated temperatures, high temperature driven ROS accumulation in elongating pollen tubes was observed in both VF36 and *are* but was absent in *are-F3H*-T5 and VF36-*F3H*-T3 (Figure 5D). These results are consistent with elevated ROS in a mutant impaired in synthesis of flavonol antioxidants. This finding also sheds light on the mechanism for the enhanced thermotolerance of the *are-F3H*-T5 and VF36-*F3H*-T3 lines as temperature-induced ROS increases can be mitigated through increased production of flavonol antioxidants.

Exogenous flavonols reduce the effect of heat stress on germination and tube length of VF36 and *are* pollen

The data described above reveals the positive effect of endogenously synthesized flavonols on maintaining ROS homeostasis, improved pollen yield, viability, germination, and tube growth, especially under temperature stress. However, this data does not reveal which flavonols have this effect, at what stage flavonols function, and whether exogenous flavonols can be taken up by pollen to reverse the *are* phenotypes. To further demonstrate that the impaired germination in the *are* mutant is tied to reduced flavonol levels and to ask whether specific flavonols confer protection to pollen, we performed chemical complementation of *are* using exogenous flavonols.

We utilized the flavonols kaempferol, quercetin, and myricetin, whose synthesis occurs in the biosynthetic pathway after the F3H enzyme, which is nonfunctional in *are* (Figure 1). We harvested pollen grains and placed them in PGM containing solvent or flavonols at doses of 5 and 30 μM and assessed germination after 30 minutes at 28 or 34°C. Chemical supplementation with 5 μM kaempferol reversed the impaired pollen germination in *are* at 28°C to levels

equivalent to VF36. Kaempferol also significantly improved the germination of *are* pollen at 34°C. Additionally, kaempferol was also able to protect VF36 from temperature-impaired germination with VF36 germination at 34°C significantly increased with treatment with either 5 or 30 µM kaempferol from 62% in untreated controls to 80%. We also examined the effect of treatment with similar doses of quercetin and myricetin and found that both of these flavonols also restored germination in *are* to wild-type levels and reduced the effect of elevated temperatures in both VF36 and *are* (Supplemental Figure 3). The new findings that even grains detached from the flower are still protected from heat stress by flavonols suggest that flavonols function specifically within pollen grains and that all 3 flavonols can protect mature pollen from temperature stress. This broad action of all 3 flavonols differs from other cases were specific flavonols have unique functions, such as in the control lateral root and root hair formation in Arabidopsis (Gayomba and Muday, 2020; Chapman and Muday, 2021).

We examined the ability of exogenous flavonols to enter pollen and scavenge ROS within the grains by incubating *are* and VF36 in PGM supplemented with kaempferol at 0, 5, or 30 µM at optimal and elevated temperatures and visualized ROS in pollen grains with CM-H_2DCFDA as described above. Treatment with exogenous kaempferol did not alter DCF levels in VF36 grains at either concentration at 28°C, though both concentrations were able to significantly decrease DCF levels in *are* at this temperature when compared to untreated controls (Figure 6B). In pollen germinated at 34°C, kaempferol at both 5 and 30 µM was also able to diminish the elevated DCF intensity in both VF36 and *are* pollen grains.

Inhibition of respiratory burst oxidase homolog (RBOH) enzymes prevented heat stress induced ROS and impaired pollen tube elongation

We tested the hypothesis that elevated ROS in response to temperature stress was mediated by NADPH oxidase/RBOH enzymes. RBOHs are plasma membrane localized enzymes that produce superoxide in the extracellular space. Superoxide can be converted to hydrogen peroxide by way of superoxide dismutase (SOD) and enter cells via aquaporins (Chapman et al., 2019). Consistent with this enzyme being made in pollen, we examined an RNA Seq dataset (described below) and identified two RBOH genes (*SlRBOHE* and *SlRBOHH*) whose transcripts are expressed in tomato pollen, with *SlRBOHH* being the most highly expressed of the two (Supplemental Table 2). Intriguingly, temperature stress did not result in

increased expression of either of these RBOHs, suggesting that their activity may be regulated post-transcriptionally.

We used VAS2870, a highly specific inhibitor of mammalian RBOH activity (Reis et al., 2020) that also inhibits plant RBOH enzymes (Postiglione and Muday, 2022) and examined the ability of this inhibitor to reduce ROS and to enhance pollen tube germination and elongation. We germinated pollen grains from VF36 and *are* flowers in PGM containing 1 μM VAS2870, or in PGM with a solvent control for 30 min at 28°C. Pollen was then transferred to 34°C or kept at 28°C for an additional 90 minutes and then labeled with CM-H_2DCFDA for 20 minutes (Figure 7A). Treatment of VF36 pollen with VAS2870 during the 28°C incubation did not alter the levels of DCF fluorescence. In contrast, at elevated temperatures, the 2.2-fold increase in DCF fluorescence in VF36 at 34°C relative to 28°C was blunted after inhibitor treatment (Figure 7B). We also observed significant decreases in DCF fluorescence in VAS2870 treated *are* pollen tubes at both 28°C and 34°C. These results are consistent with the ROS increases at elevated temperature being driven by increased activity (but not synthesis) of RBOH enzymes in pollen.

This reduction in temperature-dependent ROS synthesis in pollen tubes treated with VAS2870 was also reflected by decreased temperature effects on the length of pollen tubes. VF36 and *are* exhibited a 1.3-fold and a 1.5-fold increase, respectively, in pollen tube length at 34°C as compared to tubes in each genotype without inhibitor (Figure 7C). However, the disruption of ROS synthesis did not increase pollen tube length in VF36 at 28°C, but rather led to a 1.5-fold reduction in the length of tubes incubated with VAS2870. This result is consistent with a requirement for RBOH mediated ROS synthesis at the tip of pollen tubes that are required for tip growth as shown using mutants in both Arabidopsis and tomato (Potocký et al., 2007; Kaya et al., 2014; Jiménez-Quesada et al., 2016; Dai et al., 2021). These results indicated that ROS synthesis in this genotype may have been decreased to suboptimal levels for successful tube extension.

We also examined the effects of RBOH inhibition during heat stress on pollen germination rates. Incubation with VAS2870 did not affect VF36 germination at either temperature, but treatment with this inhibitor significantly improved germination of *are* pollen grains by 1.2-fold at 28°C and 1.6-fold at 34°C (Figure 7D). These findings are consistent with

RBOH enzymes driving elevated ROS synthesis in response to temperature stress and as the source of damaging ROS that impairs pollen tube growth.

At elevated temperatures, the *are* mutant has more differentially expressed genes than VF36 and VF36-*F3H*-T3

To provide insight into the mechanisms by which flavonols and elevated temperatures, individually or jointly, control pollen tube germination and elongation, we performed a time-course RNA-Seq analysis using VF36, *are,* and VF36-*F3H*-T3. For each line, mRNA was collected from pollen at 15 and 30 minutes of gemination at either 28°C or 34°C, representing the pollen germination phase. Additionally, we collected mRNA samples from pollen tubes that were germinated at 28°C for 30 min and then either kept at that temperature or transferred to 34°C for an additional 45 or 75 min (75 or 105 minutes of total growth), representing the pollen tube elongation phase (Supplemental Figure 4). These time points are when *are* had impaired pollen germination and pollen tube growth and elevated ROS levels as indicated by light microscopy of pollen morphology and DCF fluorescence, respectively.

RNA was then isolated for each sample and samples were shipped for paired-end, strand-specific RNA sequencing. We uploaded the reads of all samples into Integrated Genome Browser (Freese et al., 2016) and examined the *F3H* gene (*PRAM_26184.1* in tomato genome version SL5*,* formerly *solyc02g083860* in genome version SL4), we verified the presence of the *are* point mutation, which is in the 47,450,716 position in the *F3H* gene in which a C is replaced with a T (Supplemental Figure 5). This mutation is absent in all other samples.

We conducted a principal component analysis (PCA) plot using the top 500 most variable samples to investigate similarities in the transcriptome-wide expression profiles (Figure 8A). Principal component 1 (PC1) explains 58% of the variance in expression profiles and clearly separates the *are* samples from VF36 and VF36-T3 samples. PC2 explains 18% of the variance and clearly separates samples by time and temperature stress, with later time points and higher temperature stress in all three genotypes distinct from earlier and non-heat stressed samples. Analysis of *are* samples separately shows a strong PC1 (69% explained) that again correlates with time and temperature (Figure 8B). Similarly, analyses of VF36 and VF36-T by themselves separate on PC1 by time and PC2 by elevated temperature (Figure 8C,D). This difference is

accentuated in the time points taken during the pollen tube elongation phase, which were exposed to the 34°C temperature for 45 or 75 minutes.

Differentially expressed genes (DEGs) significant at adjusted $P < 0.05$ and $\log_2$-fold change of greater than or less than 1 between 28°C and 34°C increased over the time course, with at least twice as many DEGS detected in *are* than VF36 or VF36-T3 at every time point (Figure 9A). Differential gene expression analysis of the 75-minute pollen tube samples at 34°C to 28°C for *are,* VF36, and VF36-T3 detected only DEGs that were upregulated at the higher temperature in all three genotypes (Figure 9B-D). This pattern of a strong majority of significant DEGs being upregulated is similarly found at all time points (Supplemental Figures 6–8).

We generated volcano plots of VF36, *are,* and VF36-*F3H*-T3 at all four time points. The DE genes within genotype in 34°C samples relative to 28°C samples are shown at the 75-minute time point (105 minutes total growth) (Figure 9B-D). These volcano plots demonstrate that the majority of the heat-dependent DE genes are upregulated and the greater number of DE genes in *are* than the other two genotypes. The volcano plots for all the other time points are available as Supplemental Figures 6-8. These additional plots illustrate that the majority of temperature-dependent DE genes are increased at the higher temperature across all time points.

The number and rate of transcript abundance changes are greater in *are* than other genotypes

To further compare how the heat-dependent transcriptional responses differed between *are*, VF36, and VF36-T3, we determined how many DE genes were shared between these genotypes. For this comparison we evaluated the significant DEGs based on temperature at the 75 min timepoint (105 min total growth), as this timepoint contained the largest number of DEGs. The UpSet plot in Figure 10A shows that the largest group of DEGs are 74 *are*-specific DEGs, followed by 41 DEGs shared among all three genotypes, after which the DEG overlaps are trivially smaller (Figure 10A). This result illustrates that a strong majority of VF36 andVF36-T3 DEGs were also differentially expressed in *are*, but that *are* also had a substantial number of additional DEGs not found in VF36 orVF36-T3.

Functionally, DEGs for the 34°C-28°C contrast at 75 minutes were enriched in Gene Ontology (GO) annotation for "response to stress," "response to heat," and other GO categories relating to H_2O_2, as expected given the experimental treatment and our biochemical results that showed the treatment elevated ROS. The other enriched GO terms include "protein folding," "protein complex formation," and "chaperone dependent protein folding," which reflect the expected synthesis of proteins that function to reduce the effects of heat that denatures proteins. The notable number of *are*-specific temperature-responsive DEGs is accompanied by several *are*-specific functional enrichments, such as "protein-containing complex assembly," "protein complex oligomerization," "chaperone cofactor-dependent refolding," and "response to hydrogen peroxide" (Figure 10B). The *are*-specific DEGs also include a variety of antioxidant enzymes belonging to the glutathione-S-transferase, ascorbate peroxidase, and thioredoxin families, a very intriguing finding that may indicate an alternative mechanism of ROS homeostasis are activated in *are* pollen to compensate for the lack of flavonol antioxidants.

To determine if there were genotype-specific differences in the heat stress response of temperature responsive DEGs, we calculated the $\log_2$-fold change ($\log_2$FC) at 34°C relative to the 28°C sample for each timepoint and then evaluated transcripts that were DE in at least two genotypes at the 75 min time point (105 min total growth). In the 56 DEGs found in two or more genotypes, it is evident that they are upregulated more rapidly and to a higher magnitude in *are* than in VF36 and VF36-T3. Notably, most DEGs are regulated similarly in VF36 and VF36-T3 with few unique genes in either genotype, suggesting the improved pollen performance seen in VF36-T3 is not based on a differential regulation in response to heat. On the other hand, *are* contains a large number of unique genes that were not found to be differentially regulated in the other two genotypes (Figure 10A). This group of genes may yield important candidates for future targets to prevent the damaging effects of elevated temperatures.

We also examined the transcriptional regulation of the *F3H* gene in *are* and VF36 pollen. Intriguingly, *F3H* expression was elevated in *are* when compared to VF36 and VF36-*F3H*-T3 at all time points and temperatures (Supplemental Table 2). This is consistent with the point mutation in *are* producing a full transcript, and with the absence of a flavonol intermediate that acts as a negative feedback signal to decrease *F3H* transcription. Together, these data indicate

that heat-driven transcriptional responses in tomato pollen differ with levels of flavonols, as well as the length of exposure to increased temperature.

Pollen from *are* exhibits a differential transcriptional baseline than VF36

Our finding of increased transcriptional response of *are* to heat stress provides greater insight into the poor performance of pollen from this genotype at elevated temperatures. However, this analysis does not explain the impaired pollen performance observed in *are* at optimal temperatures. To understand how *are* differs from its parental line at each time point and temperature, another DE analysis was performed comparing VF36 to *are* at each developmental time point and temperature. This comparison revealed consistent differences in transcript abundance between these genotypes at all pollen developmental stages across this time course. Across the time course, we found 20 *are*-specific DEGs in common among all time points, with a maximum of 79 at 34°C at two time points (Supplemental Table 3). As shown here in other analyses, genotype-dependent DEGs increased with elevated temperature, particularly at the later stages of the time course. The relative abundance of transcripts in *are* relative to VF36 was calculated for the 20 DEGs that had significant differences at all 4 time points, with a majority of these genes having higher abundance in *are* (Supplemental Figure 12). We also examined a core set of genes encoding 36 heat shock proteins, heat shock transcription factors, or molecular chaperones that were temperature-dependent DEGs within each genotype (shown in Figure 10C). We calculated the $\log_2$FC for these genes when the transcript abundance at 28°C in *are* was reported relative to VF36 in time and temperature matched samples (Figure 11). Of these 36 genes, 29 were upregulated in *are* pollen at optimal temperatures at all developmental stages beginning with the 15-minute timepoint. This analysis suggests that, even at a near-optimal 28°C, *are* contains a different transcriptional setpoint than VF36 and *are* pollen transcriptionally reflects the stress of elevated ROS and the resulting protein unfolding.

DISCUSSION

Exposure of plants to temperatures above the optimal range can have a deleterious effect on multiple stages of reproductive and vegetative growth and development, resulting in critical reductions in crop yield at elevated temperatures (Sato et al., 2006; Fahad et al., 2017; Rieu et al., 2017; Begcy et al., 2019; Chaturvedi et al., 2021). An increase of as little as 4-6°C above

optimal temperatures during pollen germination and tube elongation both increases reactive oxygen species (ROS) and reduces pollen performance (Muhlemann et al., 2018; Wu et al., 2020). While localized, temporally-coordinated ROS bursts are required at each stage of pollen growth and development (Potocký et al., 2007; Johnson et al., 2019; Daryanavard et al., 2023), ROS overaccumulation at inappropriate development stages can reduce crop yield (Mittler, 2002; Speranza et al., 2012; Muhlemann et al., 2018). Plants synthesize antioxidant proteins and specialized metabolites, including flavonols, as a protective measure against these damaging ROS changes, and mutants that make no flavonols have impaired or failed reproduction (Schijlen et al., 2007; Muhlemann et al., 2018; Wang et al., 2020; Daryanavard et al., 2023). Muhlemann et al. (2018) reported that the impaired pollen performance of *are* at optimal temperatures was reversed by complementation with an *F3H* transgene, showing that pollen germination, tube elongation, and tube integrity, as well as ROS levels, were restored to wild-type levels (Muhlemann et al., 2018). This article evaluated the hypersensitivity of *are* to elevated temperature and asked whether flavonols protect a broad range of pollen processes, including pollen development, germination, and tube extension, from the negative effects of heat stress by examination of a complemented mutant line and plants engineered to overproduce flavonols or treated with exogenous flavonols. We examined temperature effects on ROS levels in each of the genotypes and treatments to determine if the protection conveyed by flavonols is to maintain ROS homeostasis. Finally, we asked whether heat dependent changes in the pollen transcriptome were amplified in *are*, consistent with elevated ROS driving transcriptome remodeling.

We examined pollen temperature responses using the tomato mutant *anthocyanin reduced* (*are*), which contains a point mutation in the gene encoding the flavanone 3-hydroxylase (F3H) enzyme. This mutant has reduced synthesis of flavonoids including flavonols and the downstream metabolites, anthocyanins (Maloney et al., 2014). The *are* mutant has alterations in root development including reduced lateral root formation and increased root hair formation (Maloney et al., 2014) as well as altered guard cell closure in response to ABA treatment (Watkins et al., 2017), with aspects of both of these phenotypes tied to higher level of ROS in the *are* mutant. The performance of *are* pollen is impaired in optimal growth conditions, resulting in a significant reduction in seed set when compared to VF36, its parental line (Muhlemann et al., 2018). Previous studies in rice, tomato, and petunia have also found that mutations that disrupt flavonol biosynthesis impaired pollen development and function, as well as reduced fruit yield

and seed set (Mo et al., 1992; Schijlen et al., 2007; Wang et al., 2020). A recent paper also found that the Arabidopsis *tt4* mutant, which makes no flavonols also has impaired performance at elevated temperature (Xue et al., 2023). The molecular mechanisms by which heat stress leads to impaired pollen performance, the effects that flavonols play in the alteration of these mechanisms, and whether increased flavonol synthesis can be used as a strategy to enhance pollen growth and development during exposure to elevated temperatures were not previously reported.

We evaluated the effects of flavonols on pollen yield, as well as pollen viability when exposed to temperature stress. The *are* mutant contained a significant reduction in the number of viable pollen grains when compared to VF36 at both optimal temperatures (28°C) and after a 2-hour exposure to heat stress (34°C) resulting in only 4% of *are* grains being viable, while 51% of the grains from the parental line were able to survive this temperature stress. Additionally, we examined the effect of a 30 min treatment at these two temperatures on pollen germination, revealing that only 44% of *are* pollen grains germinated at the elevated temperature, while 62% of VF36 germinated. Premature pollen tube rupture was also increased in *are* at elevated temperature relative to VF36, in co-culture experiments using either genotype marked with a LAT52-GFP pollen reporter. We also evaluated pollen tube elongation to find that *are* displayed 1.3-fold shorter tubes at 28°C and a 1.2-fold decrease in tube length at 34°C relative to VF36 at these same temperatures. These results highlight how diminished flavonol synthesis results in impaired pollen production, germination, tube extension and that these aspects are critically impaired with elevated temperature.

To demonstrate that this impaired pollen production and germination in *are* were directly tied to flavonol levels in these genotypes, and whether exogenous application of flavonols could enhance pollen heat tolerance, we incubated both *are* and VF36 with the three most prevalent flavonols in tomato: kaempferol, quercetin, and myricetin. As little as 5 μM of each flavonol was able to reverse the impaired germination in *are*, with the most profound effects evident in the presence of temperature stress. These findings are consistent with a previous report utilizing a petunia *chs* mutant that showed that chemical complementation with these three same flavonols at optimal temperatures partially rescued pollen germination (Mo et al., 1992), with kaempferol being the most potent at restoring germination with chemical supplementation (Pollak et al.,

1993). This study is the first to show that chemical application of flavonols to tomato pollen can confer heat tolerance and reverse the temperature hypersensitivity in a mutant with impaired endogenous flavonol synthesis.

The effect of genetic complementation of the *are* mutant and overexpression of the *F3H* gene on pollen performance was also examined. Previously *are* was transformed with an *F3H* gene driven by the constitutive CaMV-35S promoter, with the line *are-F3H*-T5 (*are*-T5) being the best characterized transformation, as well as the VF36-*F3H*-T3 (VF36-T3) line transformed with this same construct to overproduce flavonols (Maloney et al., 2014). We utilized these same lines and demonstrated that genetic complementation rescued the impaired pollen performance in *are*, especially at elevated temperatures. Pollen of the *are-F3H*-T5 transgenic lines showed improved yield, viability, germination, and tube growth when compared to *are*, resulting in performance that was similar to or better than wild-type pollen, consistent with the reduced levels of flavonols being causative of the pollen performance defects. Of greatest note, transformation with an *F3H* gene in VF36 resulted in protection of pollen from temperature stress in these same assays, resulting in substantially higher viability, germination, tube growth, and pollen tube integrity than in VF36.

We asked whether flavonols are protecting pollen from heat stress through their action as antioxidants (Daryanavard et al., 2023) by examining ROS levels in *are*, VF36 and the *are-F3H*-T5 line using the general ROS indicator CM H_2DCF-DA, which is oxidized by multiple forms of ROS to become the fluorescent product DCF. At both elevated and optimal temperatures, *are* pollen showed elevated DCF fluorescence in both pollen grains and tubes relative to VF36 pollen. Both genotypes had elevated ROS at 34°C compared to their 28°C controls, with *are* pollen at 34°C having the highest overall DCF fluorescence intensity. The accumulation of ROS in germinating pollen grains and elongating tubes in *are*-T5 was reduced at both 28°C and 34°C relative to *are* at those same temperatures and relative to VF36 at 34°C. Additionally treatment with kaempferol had a similar effect on ROS levels and pollen germination. These results demonstrate that both genetic and chemical complementation reversed the effect of the *are* mutation on ROS accumulation and pollen performance and even raised germination to levels that were more optimal than in the VF36 parental line under heat stress. These observations suggest that the impairments in VF36 at elevated temperatures and the reductions in pollen

germination and tube elongation in *are* at both temperatures were due to the overaccumulation of ROS.

The ability of the VF36-*F3H*-T3 line to be insensitive to the effects of high temperature on pollen viability, germination, and tube growth and to maintain constant levels of ROS at elevated temperatures during the pollen germination and pollen tube elongation phases, are exciting results. These findings provide evidence for the mechanism by which the *F3H* transgene enhances thermotolerance when exposed to high-temperature stress. Collectively, these data suggest that increasing flavonol biosynthesis reduced levels of ROS to protect pollen from oxidative damage, which may have applications in breeding or engineering crops to protect pollen from temperature-induced ROS and the resulting impairments to pollen performance. We also evaluated whether the inhibition of enzymatic drivers of ROS synthesis would be able to block temperature-stress induced ROS. ROS can be produced by many sources, including electron transport in metabolic organelles and enzymes such as Respiratory Burst Oxidase Homologs (RBOH)/NADPH Oxidase (NOX) (Møller et al., 2007; Martin et al., 2022; Postiglione and Muday, 2022). We detected transcripts encoding two RBOH enzymes that are expressed in tomato pollen. Previous results indicate that RBOHs function in multiple stages of pollen growth using both Arabidopsis mutants and chemical inhibition with DPI, a nonspecific flavoprotein inhibitor (Potocký et al., 2007; Speranza et al., 2012; Kaya et al., 2014; Jiménez-Quesada et al., 2016; Muhlemann et al., 2018; Jimenez-Quesada et al., 2019).

Therefore, we asked whether temperature-induced ROS acted via RBOH enzymes by incubating pollen with the selective, pan-RBOH inhibitor, VAS2870, which targets an active-site cysteine that is conserved across mammalian NOX enzymes as well as RBOHs in plants (Yun et al., 2011), providing increased specificity over other inhibitors such as DPI (Mangano et al., 2017; Postiglione and Muday, 2022). RBOH inhibition blunted the increased ROS accumulation after incubation at 34°C in pollen tubes in our four core genotypes. This inhibitor reduced the negative effect of high temperature on pollen tube length when compared to pollen at elevated temperature that did not receive the inhibitor. VAS2870 treatment reduced formation of elevated ROS by high temperatures, improving impaired pollen germination and tube length under these circumstances.

To better understand the molecular mechanisms by which temperature affected the function of germinating pollen grains and elongating pollen tubes, we examined the transcriptome in VF36, *are*, and the VF36-*F3H*-T3 transgenic line at optimal and elevated temperatures at four time points during pollen germination (15 or 30 min after hydration) and pollen tube elongation (75 and 105 minutes after hydration) reflecting the peak rate of pollen tube elongation. We identified differentially expressed (DE) transcripts at 34°C as compared to 28°C in all genotypes, revealing that the number of DE genes was substantially higher in *are*. There were increasing number of DE transcripts in pollen grains and tubes as the duration of the heat stress period increased. There was a large group of DE genes that were shared between all genotypes with almost all of them increasing with elevated temperature, with heat maps revealing the greater rate and magnitude of these responses in *are*. Among these shared DE genes are multiple heat shock proteins, chaperones, and heat shock transcription factors, who have significantly enriched annotations as revealed by a GO annotation analysis. These groups of DE genes are, consistent with the previously reported transcriptional response to heat stress in tomato pollen (Frank et al., 2009). The differential remodeling of the transcriptome of male reproductive tissues after exposure to elevated temperatures between tomato lines with different levels of thermosensitivity is in agreement with a prior report evaluating the transcriptome of meiotic anthers (Bita et al., 2011).

We did identify a large number of DE transcripts that were increased in *are* in response to heat stress, but not in VF36 or VF36-*F3H*-T3, which is most evident in the UpSet plot in Figure 10. We also found that the DE genes in *are* also had enriched annotations not found in the other genotypes including chaperone cofactor-dependent refolding and response to hydrogen peroxide, suggesting an enhanced temperature stress effect in *are* pollen. These responses may be linked to the elevated ROS in *are*, which through oxidation of cysteine residues to form cysteine sulfenic acids can reversibly oxidize proteins to alter their structure (Garrido Ruiz et al., 2022) compounding the effect of elevated temperature on protein denaturation.

To explore whether there are differential transcriptional responses in *are* in the absence of temperature stress, we performed a DE analysis between *are* and VF36 at all time points and temperatures. This analysis revealed a group of genes that were DE at all timepoints and temperatures, with increasing number of DE genes between genotypes at 34°C, consistent with

the greater temperature dependent increases in DE genes in *are* when comparisons were made within genotypes. When comparing the transcriptional baselines of *are* to VF36 at optimal temperatures, we identified a group of 36 genes that are involved in the heat stress response and are upregulated in *are* as early as the 15-minute timepoint. This finding suggests that *are* pollen may have altered protein folding due to elevated ROS even at optimal temperatures leading to impaired pollen performance in *are* even at 28°C.

These results reveal that an increase of flavonol levels above wild-type levels can act as a novel avenue to protect tomato pollen from the deleterious effects of elevated temperature stress. Consistent with this finding, a 2-fold increase in flavonols was detected in tomato pollen after growth at 38ºC has been reported (Paupière et al., 2017), and pollen of two tomato cultivars Saladette and CLN1621, had increased pollen viability under heat stress, and had 2-fold higher levels of flavonols than thermosensitive Money Maker and M82 (DINAR and RUDICH, 1985; Firon et al., 2006; Xu et al., 2017). suggesting that plants may produce flavonols to protect against temperature induced ROS.

We showed that diminished flavonol synthesis in a tomato mutant, such as *are*, critically reduces tolerance to elevated temperatures in pollen reducing both pollen performance tied to elevated levels of ROS consistent with the reduced levels of flavonol antioxidants. These temperature-dependent effects can be rescued with both exogenous flavonol treatment as well as engineering plants with the *F3H* transgene to increase flavonol biosynthesis and protect pollen from heat stress. We also demonstrated a role for RBOH enzymes in temperature-dependent ROS synthesis. Additionally, our data reveal a robust transcriptional response to elevated temperatures that is accentuated by reduced levels of flavonols in pollen grains and tubes and may provide additional candidate genes to improve thermotolerance in crop plants. Flavonols are critical for plants to adequately respond to and recover from the detrimental effects of heat stress in male reproductive tissue. Our findings provide an intriguing potential avenue to engineer crop plants with elevated flavonols to improve tolerance to elevated temperatures.

Methods and Materials

Plant material and growth conditions

Seeds of wild-type (VF36) and the *are* mutant were obtained from the Tomato Genetic Resource Center (https://tgrc.ucdavis.edu), and *35S:F3H* transgenic lines in the *are* and VF36 background including *are*-*F3H*-T5 and *are*-*F3H*-T6; VF36-*F3H*-T3 and VF36-*F3H*-T5 (abbreviated *are*-T5, *are*-T6, VF36-T3, or VF36-T5) were from (Maloney et al., 2014), where they were referred to as VF36 or *are* OE lines. The seeds of VF36 transformed with a LAT52:GFP line were from Sheilla McCormack (Zhang et al., 2008) and this transgene was crossed into are and VF36-F3H-T3 and the homozygosity of transgenes and the mutations were verified. Seeds were surface sterilized by soaking for 25 minutes in 50% bleach (v/v) followed by 4 washes with autoclaved DI water. Sterilized tomato seeds were then germinated in Sunshine MVP RSi soil and then transferred to the Wake Forest University greenhouse, where they began to flower after 6 weeks of additional growth. Pollen was also obtained from plants that were propagated by cuttings. Unless noted otherwise, all pollen was harvested from greenhouse grown seedlings with day temperatures set to 28°C and night temperature to 21°C.

Quantification of Pollen yield

Pollen from three flowers for each line were harvested as described above and placed in individual 0.7 mL microcentrifuge tubes for evaluation of pollen yield. Released pollen was resuspended in 60-µL pollen viability solution (PVS, 290 mM sucrose, 1.27 mM $Ca(NO_3)_2$, 0.16 mM boric acid, 1 mM KNO_3), then equal volume of trypan blue staining solution was added to each tube. Pollen grains were quantified by pipetting 10 µL pollen suspension into Countess cell counting chamber slides to be counted by a Countess II Automated Cell Counter (Invitrogen). Four technical replicates were taken from each tube and averaged, then pollen concentrations were calculated to reflect the total volume of solution in each tube to give the number of live pollen grains per flower.

Pollen viability assay

Pollen from three flowers at anthesis from each genotype were harvested by agitation with an electric toothbrush modified for efficient pollen harvesting into a 0.7 µL microcentrifuge tube. Pollen was then resuspended in pollen viability solution (PVS, 290 mM sucrose, 1.27 mM $Ca(NO_3)_2$, 0.16 mM boric acid, 1 mM KNO_3) which included 0.001% (wt/vol) fluorescein diacetate (FDA), and 10 µM propidium iodide (PI). Pollen grains were stained for 15 min at 28 °C and then centrifuged. PVS containing FDA and PI was replaced with PVS alone. The stained

pollen was placed on a microscope slide and imaged by confocal microscopy on a Zeiss 880 LSCM microscope. FDA was excited with a 488-nm laser and intensity was collected with an emission window of 493–584 nm. PI was excited with a 561-nm laser line while its fluorescent signal was collected within a 584–718 nm emission window. Maximum laser power was 0.7% and 0.07% for FDA and PI, respectively. Quantifications of viable and dead pollen grains were performed using Fiji in which pollen grains with FDA emission peaking at 500 nm were counted as viable and pollen with PI emission within the grain above 600 were counted as dead grains.

Pollen germination and pollen tube elongation

Flowers were collected at anthesis from greenhouse grown plants and, in most experiments, pollen was harvested as described above. In some cases, anthers were detached, and the tips of the anthers were then cut and placed into a microfuge tube and pollen was released by agitation with a vortex. Pollen was then resuspended in 300 µL of pollen germination media (PGM) (24% (w/v) PEG4000, 0.01 (w/v) boric acid, 2% (w/v) sucrose, 2 mM HEPES pH 6.0, 3 mM $Ca(NO_3)_2$, 0.02% (w/v) $MgSO_4$, 0.01% (w/v) $KNO_{3)}$, which was pre-equilibrated to either 28°C or 34°C. The entire volume of resuspended pollen was transferred into a sterile 24-well plate and imaged using an Olympus IX2-UCB inverted microscope fitted with a Tokai HIT heated stage.

For pollen germination analysis, pollen was incubated at either 28°C or 34°C for 30 minutes and images were collected every 2 minutes. Percent germination was then quantified using FIJI (ImageJ) in which the number of germinated grains were reported relative to viable mature grains, as judged by proper size, shape, and hydration. For pollen tube elongation, pollen was incubated at 28°C for 30 minutes, heat treated samples were then moved to an incubator at 34°C for 90 minutes while control samples remained at 28°C for an additional 90 minutes. Pollen tube length was measured from the tip of the pollen tube to the point of emergence on the grain.

Exogenous chemical treatments

Flavonol chemical complementation was achieved through the addition of quercetin, kaempferol, or myricetin (Indofine chemicals) to PGM at final concentrations of 1, 5, 15, or 30 µM (diluted from stock solutions of 0.1, 0.5, 1.5, 3 mM in DMSO). An equivalent volume of

DMSO was added to the controls. For VAS2870 treatment, a 50 µM stock solution (using diH_2O as a solvent) was diluted in PGM to yield a final concentration of 1 µM, while control samples received an equivalent volume of diH_2O. Pollen was resuspended in PGM equilibrated to either 28°C or 34°C containing flavonols or VAS2870 at the indicated concentrations and germination and tube length were quantified as described above.

Quantification of DCF fluorescence in pollen grains and pollen tubes

For quantification of ROS during pollen germination, pollen grains were harvested as described above and pollen was allowed to germinate for 10 minutes in PGM alone at 28°C or 34°C and then 5 µM 2'-7'-dichlorodihydrofluorescein diacetate (CM-H_2DCFDA) (Thermo-Fisher), diluted from a stock solution of 500 µM in DMSO, was added for another 20 min at 28°C or 34°C. Pollen was then centrifuged, the PGM containing CM-H_2DCFDA was removed and replaced with PGM alone, and the stained pollen was transferred to a microscope slide for imaging.

For DCF imaging of samples with elongated pollen tubes, harvested pollen was incubated at 28°C for 30 minutes. Heat treated samples were then incubated at 34°C for 90 minutes while control samples remained at 28°C. Pollen tubes were then stained with 5 µM CM-H_2DCFDA (Thermo-Fisher) for 20 min. Pollen was then centrifuged, the PGM containing CM-H_2DCFDA was removed and replaced with PGM alone, and stained pollen tubes were transferred to a microscope slide for imaging.

DCF fluorescence was visualized using a Zeiss 880 laser scanning confocal microscope (LSCM) using the 488 nm laser and an emission spectrum of 490-606 nm. Laser settings were uniform for all samples within each experiment, but for each separate experiment settings were optimized to make sure all samples were below saturating levels of fluorescence. Laser power ranged from 0.9-1.5%, a 1 Airy Unit pinhole aperture yielding a 1.2 µm section was utilized and gain ranged from 974-1034. The DCF fluorescence intensity was quantified in FIJI and each experiment was normalized to fluorescence of VF36 at 28°C.

Extraction and quantification of aglycone flavonols

For flavonol extractions, pollen was harvested, immediately frozen in liquid nitrogen and stored at -80°C until extraction. On the day of the extraction, pollen was suspended in 300 µL

pollen viability solution (PVS; 290 mM sucrose, 1.27 mM $Ca(NO_3)_2$, 0.16 mM boric acid, 1 mM KNO_3) and the number of live grains in the sample was quantified using a hemocytometer or Countess II automated cell counter (Invitrogen). The PVS was removed and replaced with 300 µL extraction buffer (containing 500 nM formononetin internal standard that was dissolved in acetone). Samples were incubated in the extraction buffer at 4°C for 20 minutes. A volume of 2 N HCl equal to the volume of the extraction buffer was added to the samples and they were incubated at 75°C for 45 min to release aglycone flavonols. An equal volume of ethyl acetate (Optima grade, Fisher) was added to the aglycone flavonols and shaken for 5 min before microcentrifugation at 17,000 x*g* for 10 min. The top organic (ethyl acetate) phase was isolated, and the ethyl acetate phase separation was repeated. The collected organic phases were pooled. Samples were dried by airflow using a mini-vap evaporator (Supelco Inc) and resuspended in 50 µl of acetonitrile before LCMS analysis.

Following resuspension in acetonitrile, samples were analyzed on a TSQ Triple Quadrupole Mass Spectrometer with an electrospray ionization source, coupled to a Thermo Accela 1250 pump and autosampler (Thermo Fisher). For analysis of flavonol extracts, 10 µl of each sample was injected on a Luna 150 x 3 mm C18 column with a Security guard precolumn with a solvent of water: acetonitrile, both containing 0.1% (v/v) formic acid. The solvent gradient was 90% water: 10% acetonitrile (v/v) to 10% water: 90% acetonitrile (v/v) in a time span of 18.5 min. From 18.5 min to 20 min, the gradient moved from 10% water: 90% acetonitrile (v/v) back to 90% water: 10% acetonitrile (v/v) and held at those concentrations for another 2 min to recondition the column. Quantification of flavonols was found by comparing the MS1 peak area data, quantified in Thermo Xcalibur, to standard curves, with concentrations of 1 µM, 500 nM, 250 nM, 125 nM, 62.5 nM, 10 nM, 5 nM, and 1 nM, generated using pure standards of naringenin, quercetin, kaempferol, and myricetin (Indofine chemicals). Total flavonol level was calculated by averaging the total flavonol value of each sample. MS2 fragmentation spectra were collected to confirm flavonol identity/structure. Fragmentation was induced using 24-41-kV collision-induced dissociation, optimized for each compound. MS2 spectra of each flavonol in plant extracts were compared with the MS2 spectra of the standards described above. The flavonol content in each sample was normalized to the number of live grains in the sample and reported in units of fmoles/10000 grains.

Pollen sample preparation and RNA isolation for sequencing

Pollen was harvested as described above from VF36, *are,* and VF36-*F3H*-T3 using 4-7 flowers of VF36 and VF36-T3 and three times as many flowers from *are* to result in similar yields of pollen across genotypes. For the 15- and 30-minute timepoints, pollen was resuspended in 100 µL PGM equilibrated at 28°C. For each genotype, 20 µL of pollen suspension was then transferred to 4 separate 1.5 mL microcentrifuge tubes containing 980 µL of PGM equilibrated at either 28°C or 34°C (15- and 30-minute timepoints at 28°C and matching timepoints at 34°C) and incubated in water baths set to the corresponding temperatures. An additional 5 µL from each pollen suspension was also transferred to two 24-well plates, equilibrated at 28°C or 34°C, to be imaged live as described earlier for the evaluation of pollen germination. For each replicate we verified that the impaired pollen performance of *are* and robust pollen performance of VF36-T3 were evident as judged by pollen tube integrity and growth. Pollen was incubated at either 28°C or 34°C for 15 minutes, then samples for the corresponding timepoint were removed and pelleted by centrifugation at 10,000x *g* for 1 minute. Supernatant PGM was removed from each tube until only the pellet remained and pollen samples were flash frozen in liquid nitrogen. The same procedure was repeated for the 30-minute timepoint after the completion of incubation.

For the 45- and 75-minute timepoints, pollen was resuspended in 100 µL PGM equilibrated to 28°C. For each genotype, 20 µL of pollen suspension was then transferred to 4 separate 1.5 mL microcentrifuge tubes containing 980 µL of PGM that were all equilibrated to 28°C and incubated in the 28°C water bath for 30 minutes. An additional 5 µL from each pollen suspension was also transferred to two 24-well plates that were equilibrated to 28°C, to be germinated for 30 minutes. After 30-minute incubation at 28°C, two microcentrifuge tubes from each genotype were transferred to the 34°C water bath to be incubated for an additional 45- or 75-minutes while the other two tubes remained at 28°C. One 24-well plate was also transferred to 34°C to be imaged live as described earlier for the evaluation of pollen tube elongation. Pollen was incubated at either 28°C or 34°C for 45 additional minutes (75 minutes total growth), then samples for the corresponding timepoint were removed and pelleted by centrifugation at 10,000x *g* for 1 minute. PGM was removed from each tube until only the pellet remained and pollen samples were flash frozen in liquid nitrogen. The same procedure was repeated for the 75-minute timepoint (105 minutes total growth) after the completion of incubation.

Pellets were pulverized using sterile micropestles in liquid nitrogen (Thermo-Fisher), and RNA isolation was completed in accordance with the Qiagen plant RNeasy kit protocol (Qiagen). DNA was removed via off-column DNase treatment with the RapidOut DNA Removal Kit (Thermo Scientific). Concentrations for each sample were quantified via a Nanodrop spectrophotometer (Thermo-Fisher) after initial RNA isolation and again following DNase treatment. Each sample contained at least 1.5 µg of RNA. GENEWIZ, LLC (Azenta Life Sciences) completed paired-end, strand-specific RNA sequencing through utilization of the Illumina HiSeq platform.

Analysis of RNA Seq samples

All analysis and data processing code, along with documentation and RNA-Seq "counts" data files, are available from the project "git" repository https://bitbucket.org/hotpollen/flavonoid-rnaseq. The raw read files are available in the NCI: Sequencing Read Archive (SRA) under the project name: SRP460750. The RNA sequencing data was processed through the nf-core/rnaseq pipeline version 3.4 (Ewels et al., 2020). Sequences were aligned to the two most recently published tomato genome assemblies and annotation sets, designated SL4/ S_lycopersicum_Sep_2019 and SL5/ S_lycopersicum_Jun_2022 (Zhou et al., 2022) using the Salmon/STAR option settings (Dobin et al., 2012) for the nf-core/rnaseq pipeline. All gene IDs utilized in the text or in figures refer to the SL5 version of the tomato genome. The pipeline produced RNA-Seq to genome assembly alignment files, one per input library. To enable visual detection of differential expression across samples, we further processed the alignment files using the "bamCoverage" function from deepTools, a suite of command-line programs for processing and analyzing RNA-Seq and other high-throughput sequence datasets (Ramírez et al., 2016). This produced scaled coverage graphs reporting the number of aligned RNA-Seq fragments per genomic base pair position, scaled by library sequencing depth, allowing visual comparison of expression levels across samples. To enable visualization and assessment of splicing patterns, FindJunctions (https://bitbucket.org/lorainelab/findjunctions/) was used to create "BED" format files reporting the genomic coordinates of introns inferred from the data and the number of alignments supporting the discovered intron. The RNA-Seq alignment, coverage graph, and junction files were deployed to an IGB Quickload site for visualization in the Integrated Genome Browser (IGB) (Freese et al., 2016). Code used to create the IGB Quickload

site, along with instructions on how to use IGB to view and explore the data, are available from https://bitbucket.org/hotpollen/genome-browser-visualization.

In addition to RNA-Seq alignment files, the nf-core/rnaseq pipeline produced a gene expression counts table reporting the number of RNA-Seq fragments observed per gene, per sample, with each column representing a different experimental sample consisting of different time, temperature, genotype, and replicate. The time course consisted of two timepoints in the germination phase (15 and 30 minutes), and two time points in the pollen tube elongation phase (45 and 75 minutes of heat treatment for a total of 75 and 105 minutes of growth, respectively) at 28 or 34°C. Genotypes sequenced were VF36, VF36-*F3H*-T3, or *are*. The gene expression counts tables were provided as inputs to differential expression analysis code that used DESeq2 (Love et al., 2014) to identify differentially expressed genes either between elevated temperature treatment (34°C) and optimal (control) samples germinated at 28°C within genotype and length of growth or between genotypes at each temperature and time point. The DESeq2 model internally corrects for library size and sequencing depth. Thus, pre-processing the counts file by transforming or normalizing count-based expression values was not necessary as input. However, for visualization and validation of differential expression results, we created scaled expression data files using "counts per million" units, by dividing counts values by the total number of aligned fragments and multiplying by 1,000,000. The original counts files and derived scaled counts files are available in the code repository, along with the code used to generate them.

For exploratory visualization and clustering analysis, PCA and volcano plots were created using DESeq library function plotPCA (https://www.rdocumentation.org/packages/DESeq2/versions/1.12.3/topics/plotPCA), plotting functions from the ggplot package (https://ggplot2.tidyverse.org/), and functions from the EnhancedVolcano plot package (https://github.com/kevinblighe/EnhancedVolcano). Volcano plots were produced using the DESeq2 output comparing samples treated at 28°C to those treated at 34°C for each timepoint to explore the differentially expressed genes that are impacted by heat stress. To facilitate exploration and validation of results, RShiny apps were created that show barplots summarizing gene expression values across all samples.

Statistics

All statistical analyses of growth and fluorescence were performed using Graph Pad Prism 9 with a 2-way ANOVA followed by a Tukey post hoc test. For the quantification of flavonol abundance by LC-MS, a one-way ANOVA was used followed by a Sidak post hoc test.

Acknowledgements

The authors would like to thank the members of the Muday lab and the Genomics of Thermotolerance in Tomato (GTTR) group for their editorial input. This project was supported by the USDA-NIFA (2020-67013-30907 to GKM), NSF PGRP (IOS 1939255 to GKM, JBP, and AEL), NIH NIGMS (5R35GM139609 to AEL), and an NIH T32 (GM127261 fellowship to AEP).

References

Agati G, Azzarello E, Pollastri S, Tattini M (2012) Flavonoids as antioxidants in plants: Location and functional significance. Plant Science **196:** 67-76

Alseekh S, Perez de Souza L, Benina M, Fernie AR (2020) The style and substance of plant flavonoid decoration; towards defining both structure and function. Phytochemistry **174:** 112347

Begcy K, Nosenko T, Zhou L-Z, Fragner L, Weckwerth W, Dresselhaus T (2019) Male Sterility in Maize after Transient Heat Stress during the Tetrad Stage of Pollen Development1 [OPEN]. Plant Physiology **181:** 683-700

Bita CE, Zenoni S, Vriezen WH, Mariani C, Pezzotti M, Gerats T (2011) Temperature stress differentially modulates transcription in meiotic anthers of heat-tolerant and heat-sensitive tomato plants. BMC Genomics **12:** 384

Chapman JM, Muday GK (2021) Flavonols modulate lateral root emergence by scavenging reactive oxygen species in Arabidopsis thaliana. J Biol Chem **296:** 100222

Chapman JM, Muhlemann JK, Gayomba SR, Muday GK (2019) RBOH-Dependent ROS Synthesis and ROS Scavenging by Plant Specialized Metabolites To Modulate Plant Development and Stress Responses. Chemical Research in Toxicology **32:** 370-396

Chaturvedi P, Wiese AJ, Ghatak A, Záveská Drábková L, Weckwerth W, Honys D (2021) Heat stress response mechanisms in pollen development. New Phytologist **231:** 571-585

Considine MJ, Foyer CH (2021) Oxygen and reactive oxygen species-dependent regulation of plant growth and development. Plant Physiol **186:** 79-92

Dai X, Han H, Huang W, Zhao L, Song M, Cao X, Liu C, Niu X, Lang Z, Ma C, Xie H (2021) Generating Novel Male Sterile Tomatoes by Editing Respiratory Burst Oxidase Homolog Genes. Front Plant Sci **12:** 817101

Daryanavard H, Postiglione AE, Mühlemann JK, Muday GK (2023) Flavonols modulate plant development, signaling, and stress responses. Current Opinion in Plant Biology **72:** 102350

De Storme N, Geelen D (2014) The impact of environmental stress on male reproductive development in plants: biological processes and molecular mechanisms. Plant Cell Environ **37:** 1-18

DINAR M, RUDICH J (1985) Effect of Heat Stress on Assimilate Partitioning in Tomato. Annals of Botany **56:** 239-248

Dobin A, Davis CA, Schlesinger F, Drenkow J, Zaleski C, Jha S, Batut P, Chaisson M, Gingeras TR (2012) STAR: ultrafast universal RNA-seq aligner. Bioinformatics **29:** 15-21

Ewels PA, Peltzer A, Fillinger S, Patel H, Alneberg J, Wilm A, Garcia MU, Di Tommaso P, Nahnsen S (2020) The nf-core framework for community-curated bioinformatics pipelines. Nature Biotechnology **38:** 276-278

Fahad S, Bajwa AA, Nazir U, Anjum SA, Farooq A, Zohaib A, Sadia S, Nasim W, Adkins S, Saud S, Ihsan MZ, Alharby H, Wu C, Wang D, Huang J (2017) Crop Production under Drought and Heat Stress: Plant Responses and Management Options. Frontiers in Plant Science **8**

Falcone Ferreyra ML, Rius SP, Casati P (2012) Flavonoids: biosynthesis, biological functions, and biotechnological applications. Front Plant Sci **3:** 222

Firon N, Shaked R, Peet MM, Pharr DM, Zamski E, Rosenfeld K, Althan L, Pressman E (2006) Pollen grains of heat tolerant tomato cultivars retain higher carbohydrate concentration under heat stress conditions. Scientia Horticulturae **109:** 212-217

Frank G, Pressman E, Ophir R, Althan L, Shaked R, Freedman M, Shen S, Firon N (2009) Transcriptional profiling of maturing tomato (Solanum lycopersicum L.) microspores reveals the involvement of heat shock proteins, ROS scavengers, hormones, and sugars in the heat stress response. Journal of Experimental Botany **60:** 3891-3908

Freese NH, Norris DC, Loraine AE (2016) Integrated genome browser: visual analytics platform for genomics. Bioinformatics **32:** 2089-2095

Garrido Ruiz D, Sandoval-Perez A, Rangarajan AV, Gunderson EL, Jacobson MP (2022) Cysteine Oxidation in Proteins: Structure, Biophysics, and Simulation. Biochemistry **61:** 2165-2176

Gayomba SR, Muday GK (2020) Flavonols regulate root hair development by modulating accumulation of reactive oxygen species in the root epidermis. Development **147**

Gayomba SR, Watkins JM, Muday GK (2017) Flavonols Regulate Plant Growth and Development through Regulation of Auxin Transport and Cellular Redox Status. *In* Recent Advances in Polyphenol Research, pp 143-170

Gonzali S, Perata P (2020) Anthocyanins from Purple Tomatoes as Novel Antioxidants to Promote Human Health. Antioxidants (Basel) **9**

Groenenboom M, Gomez-Roldan V, Stigter H, Astola L, van Daelen R, Beekwilder J, Bovy A, Hall R, Molenaar J (2013) The flavonoid pathway in tomato seedlings: transcript abundance and the modeling of metabolite dynamics. PLoS One **8:** e68960

Jahan MS, Shu S, Wang Y, Chen Z, He M, Tao M, Sun J, Guo S (2019) Melatonin alleviates heat-induced damage of tomato seedlings by balancing redox homeostasis and modulating polyamine and nitric oxide biosynthesis. BMC Plant Biology **19:** 414

Jiménez-Quesada MJ, Traverso JÁ, Alché JdD (2016) NADPH Oxidase-Dependent Superoxide Production in Plant Reproductive Tissues. Frontiers in plant science **7:** 359-359

Jimenez-Quesada MJ, Traverso JA, Potocký M, Žárský V, Alché JdD (2019) Generation of Superoxide by OeRbohH, a NADPH Oxidase Activity During Olive (Olea europaea L.) Pollen Development and Germination. Frontiers in Plant Science **10**

Johnson MA, Harper JF, Palanivelu R (2019) A Fruitful Journey: Pollen Tube Navigation from Germination to Fertilization. Annual Review of Plant Biology **70:** 809-837

Kaya H, Nakajima R, Iwano M, Kanaoka MM, Kimura S, Takeda S, Kawarazaki T, Senzaki E, Hamamura Y, Higashiyama T, Takayama S, Abe M, Kuchitsu K (2014) Ca2+-activated reactive oxygen species production by Arabidopsis RbohH and RbohJ is essential for proper pollen tube tip growth. Plant Cell **26:** 1069-1080

Kovinich N, Kayanja G, Chanoca A, Riedl K, Otegui MS, Grotewold E (2014) Not all anthocyanins are born equal: distinct patterns induced by stress in Arabidopsis. Planta **240:** 931-940

Ku YS, Ng MS, Cheng SS, Lo AW, Xiao Z, Shin TS, Chung G, Lam HM (2020) Understanding the Composition, Biosynthesis, Accumulation and Transport of Flavonoids in Crops for the Promotion of Crops as Healthy Sources of Flavonoids for Human Consumption. Nutrients **12**

Lohani N, Singh MB, Bhalla PL (2019) High temperature susceptibility of sexual reproduction in crop plants. Journal of Experimental Botany **71:** 555-568

Love MI, Huber W, Anders S (2014) Moderated estimation of fold change and dispersion for RNA-seq data with DESeq2. Genome Biology **15:** 550

Maloney GS, DiNapoli KT, Muday GK (2014) The anthocyanin reduced tomato mutant demonstrates the role of flavonols in tomato lateral root and root hair development. Plant Physiol **166:** 614-631

Mangano S, Denita-Juarez SP, Choi HS, Marzol E, Hwang Y, Ranocha P, Velasquez SM, Borassi C, Barberini ML, Aptekmann AA, Muschietti JP, Nadra AD, Dunand C, Cho HT, Estevez JM (2017) Molecular link between auxin and ROS-mediated polar growth. Proc Natl Acad Sci U S A **114:** 5289-5294

Martin RE, Postiglione AE, Muday GK (2022) Reactive oxygen species function as signaling molecules in controlling plant development and hormonal responses. Current Opinion in Plant Biology **69:** 102293

Mittler R (2002) Oxidative stress, antioxidants and stress tolerance. Trends Plant Sci **7:** 405-410

Mo Y, Nagel C, Taylor LP (1992) Biochemical complementation of chalcone synthase mutants defines a role for flavonols in functional pollen. Proc Natl Acad Sci U S A **89:** 7213-7217

Møller IM, Jensen PE, Hansson A (2007) Oxidative modifications to cellular components in plants. Annu Rev Plant Biol **58:** 459-481

Muhlemann JK, Younts TLB, Muday GK (2018) Flavonols control pollen tube growth and integrity by regulating ROS homeostasis during high-temperature stress. Proceedings of the National Academy of Sciences **115:** E11188-E11197

Paupière MJ, Müller F, Li H, Rieu I, Tikunov YM, Visser RGF, Bovy AG (2017) Untargeted metabolomic analysis of tomato pollen development and heat stress response. Plant Reprod **30:** 81-94

Paupière MJ, Van Heusden AW, Bovy AG (2014) The Metabolic Basis of Pollen Thermo-Tolerance: Perspectives for Breeding. Metabolites **4:** 889-920

Pollak PE, Vogt T, Mo Y, Taylor LP (1993) Chalcone Synthase and Flavonol Accumulation in Stigmas and Anthers of Petunia hybrida. Plant Physiol **102:** 925-932

Postiglione AE, Muday GK (2022) Abscisic acid increases hydrogen peroxide in mitochondria to facilitate stomatal closure. Plant Physiology **192:** 469-487

Potocký M, Jones MA, Bezvoda R, Smirnoff N, Žárský V (2007) Reactive oxygen species produced by NADPH oxidase are involved in pollen tube growth. New Phytol **174:** 742-751

Pourcel L, Bohórquez-Restrepo A, Irani NG, Grotewold E (2012) Anthocyanin Biosynthesis, Regulation, and Transport: New Insights from Model Species. *In* Recent Advances in Polyphenol Research, pp 143-160

Pressman E, Peet MM, Pharr DM (2002) The effect of heat stress on tomato pollen characteristics is associated with changes in carbohydrate concentration in the developing anthers. Ann Bot **90:** 631-636

Raftery AE, Zimmer A, Frierson DMW, Startz R, Liu P (2017) Less Than 2 °C Warming by 2100 Unlikely. Nat Clim Chang **7:** 637-641

Raja MM, Vijayalakshmi G, Naik ML, Basha PO, Sergeant K, Hausman JF, Khan PSSV (2019) Pollen development and function under heat stress: from effects to responses. Acta Physiologiae Plantarum **41:** 47

Ramírez F, Ryan DP, Grüning B, Bhardwaj V, Kilpert F, Richter AS, Heyne S, Dündar F, Manke T (2016) deepTools2: a next generation web server for deep-sequencing data analysis. Nucleic Acids Res **44:** W160-165

Reis J, Massari M, Marchese S, Ceccon M, Aalbers FS, Corana F, Valente S, Mai A, Magnani F, Mattevi A (2020) A closer look into NADPH oxidase inhibitors: Validation and insight into their mechanism of action. Redox Biology **32:** 101466

Rieu I, Twell D, Firon N (2017) Pollen Development at High Temperature: From Acclimation to Collapse. Plant Physiology **173:** 1967-1976

Rutley N, Miller G, Wang F, Harper JF, Miller G, Lieberman-Lazarovich M (2021) Enhanced Reproductive Thermotolerance of the Tomato high pigment 2 Mutant Is Associated With Increased Accumulation of Flavonols in Pollen. Frontiers in Plant Science **12**

Sato S, Kamiyama M, Iwata T, Makita N, Furukawa H, Ikeda H (2006) Moderate increase of mean daily temperature adversely affects fruit set of Lycopersicon esculentum by disrupting specific physiological processes in male reproductive development. Ann Bot **97:** 731-738

Schijlen EGWM, de Vos CHR, Martens S, Jonker HH, Rosin FM, Molthoff JW, Tikunov YM, Angenent GC, van Tunen AJ, Bovy AG (2007) RNA Interference Silencing of Chalcone Synthase, the First Step in the Flavonoid Biosynthesis Pathway, Leads to Parthenocarpic Tomato Fruits. Plant Physiology **144:** 1520-1530

Speranza A, Crinelli R, Scoccianti V, Geitmann A (2012) Reactive oxygen species are involved in pollen tube initiation in kiwifruit. Plant Biol (Stuttg) **14:** 64-76

Torun H (2019) Time-course analysis of salicylic acid effects on ROS regulation and antioxidant defense in roots of hulled and hulless barley under combined stress of drought, heat and salinity. Physiol Plant **165:** 169-182

Wang L, Lam PY, Lui ACW, Zhu F-Y, Chen M-X, Liu H, Zhang J, Lo C (2020) Flavonoids are indispensable for complete male fertility in rice. Journal of Experimental Botany **71:** 4715-4728

Watkins JM, Chapman JM, Muday GK (2017) Abscisic Acid-Induced Reactive Oxygen Species Are Modulated by Flavonols to Control Stomata Aperture. Plant Physiology **175:** 1807-1825

Wu W, Shah F, Duncan RW, Ma BL (2020) Grain yield, root growth habit and lodging of eight oilseed rape genotypes in response to a short period of heat stress during flowering. Agricultural and Forest Meteorology **287:** 107954

Xu J, Wolters-Arts M, Mariani C, Huber H, Rieu I (2017) Heat stress affects vegetative and reproductive performance and trait correlations in tomato (Solanum lycopersicum). Euphytica **213:** 156

Xue J-S, Qiu S, Jia X-L, Shen S-Y, Shen C-W, Wang S, Xu P, Tong Q, Lou Y-X, Yang N-Y, Cao J-G, Hu J-F, Shen H, Zhu R-L, Murray JD, Chen W-S, Yang Z-N (2023) Stepwise changes in flavonoids in spores/pollen contributed to terrestrial adaptation of plants. Plant Physiology **193:** 627-642

Yoder JI, Belzile F, Tong Y, Goldsbrough A (1994) Visual markers for tomato derived from the anthocyanin biosynthetic pathway. Euphytica **79:** 163-167

Yun B-W, Feechan A, Yin M, Saidi NBB, Le Bihan T, Yu M, Moore JW, Kang J-G, Kwon E, Spoel SH, Pallas JA, Loake GJ (2011) S-nitrosylation of NADPH oxidase regulates cell death in plant immunity. Nature **478:** 264-268

Zhang D, Wengier D, Shuai B, Gui CP, Muschietti J, McCormick S, Tang WH (2008) The pollen receptor kinase LePRK2 mediates growth-promoting signals and positively regulates pollen germination and tube growth. Plant Physiol **148:** 1368-1379

Zhou Y, Zhang Z, Bao Z, Li H, Lyu Y, Zan Y, Wu Y, Cheng L, Fang Y, Wu K, Zhang J, Lyu H, Lin T, Gao Q, Saha S, Mueller L, Fei Z, Städler T, Xu S, Zhang Z, Speed D, Huang S (2022) Graph pangenome captures missing heritability and empowers tomato breeding. Nature **606:** 527-534

Figures

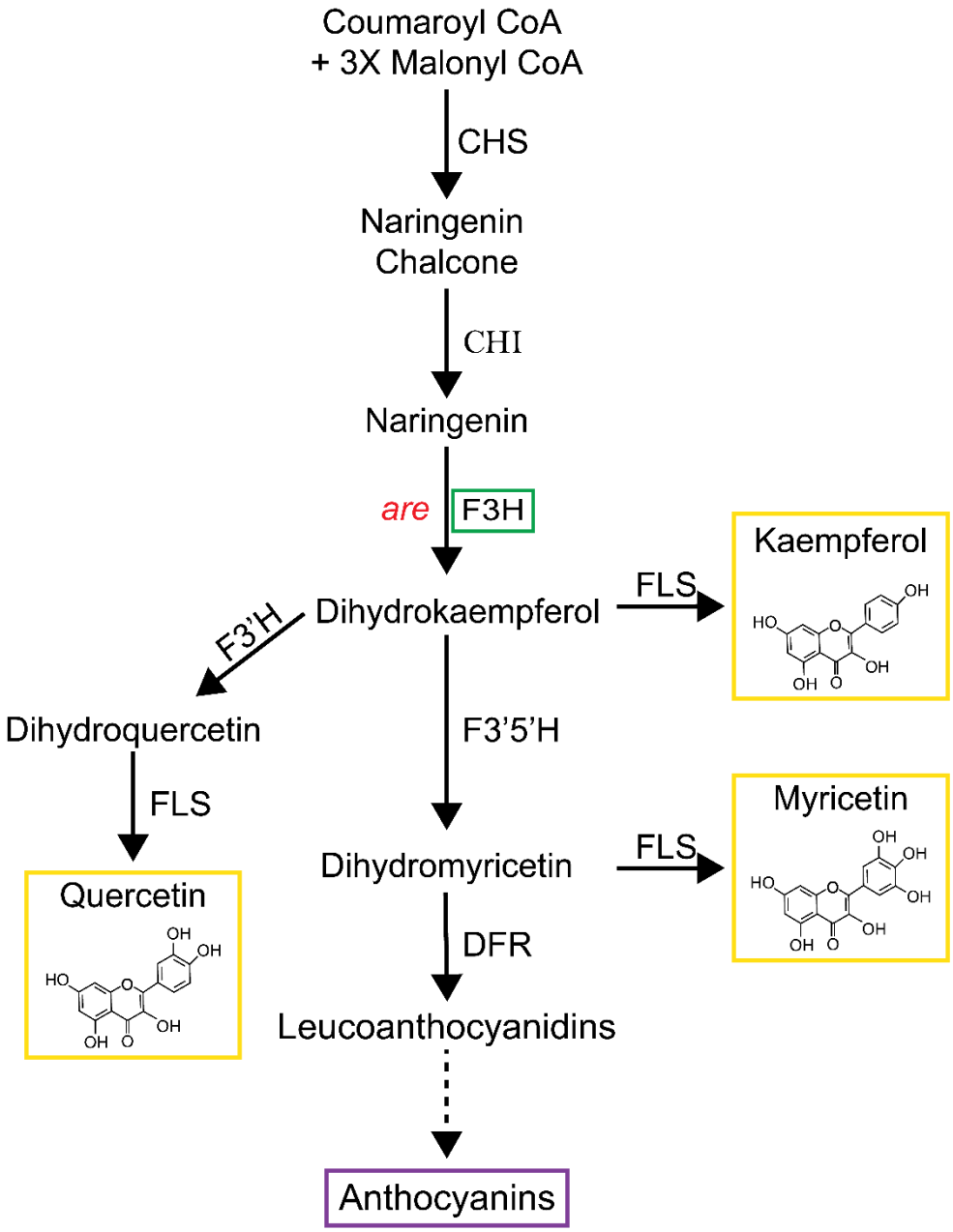

Figure 1. The flavonoid biosynthetic pathway in tomato. Pathway intermediates and enzymes that interconvert them are shown.

The major intermediates of flavonoid metabolism are indicated with the enzymes catalyzing the biosynthetic reactions are indicated. This paper focuses on the *are* mutant with a defect in the flavanone 3-hydroxylase (F3H) enzyme, indicated in the green box. The chemical structures of the most abundant flavonols in tomato are shown within the yellow box. Enzyme abbreviations are as follows: CHS: chalcone synthase; CHI: chalcone isomerase; F3'H: flavonoid 3′-hydroxylase; F3'5'H: flavonoid 3′5'-hydroxylase; FLS: flavonol synthase; DFR: dihydroflavonol reductase; ANS: anthocyanin synthase.

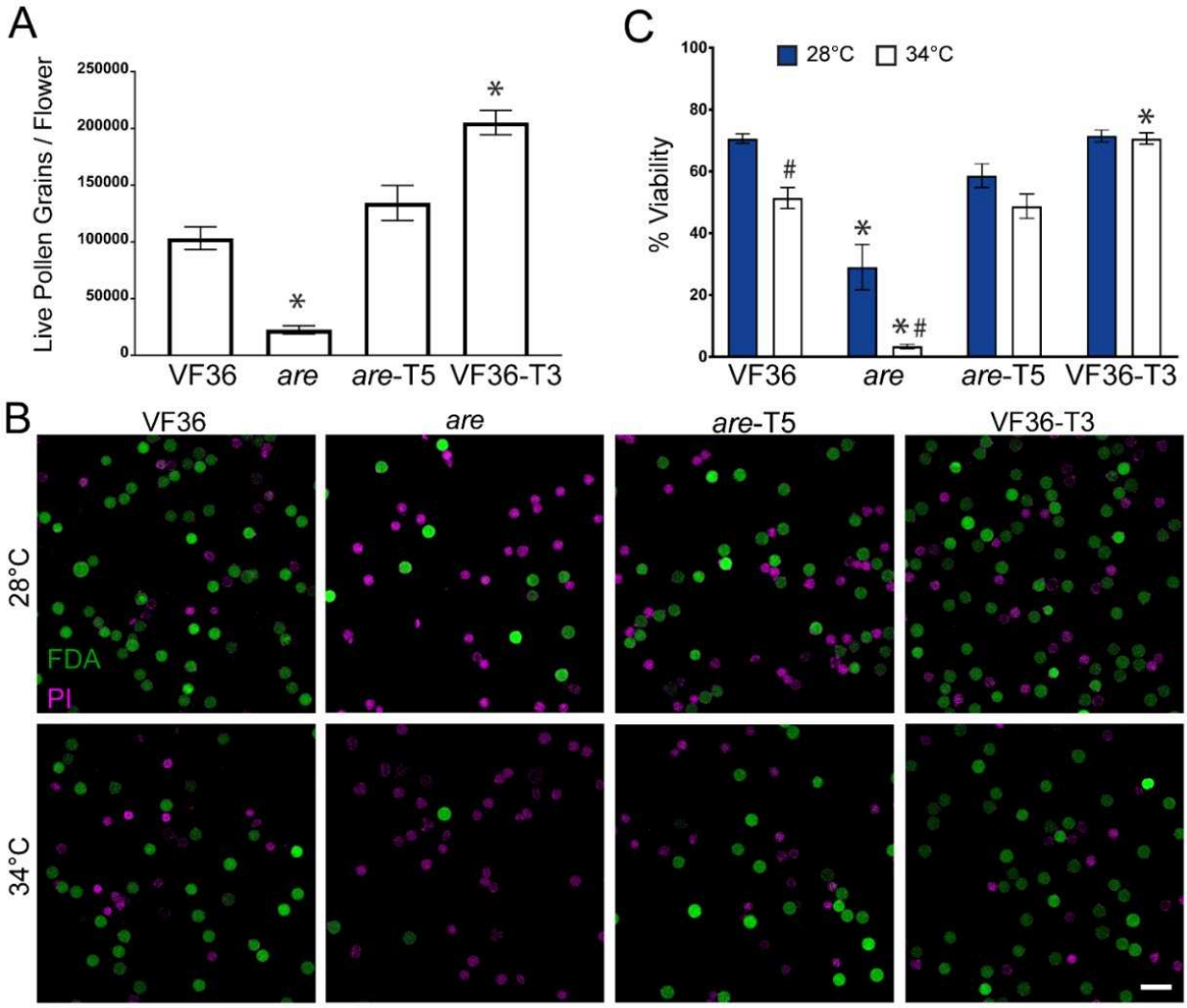

Figure 2. Flavonols positively regulate pollen yield and protect pollen viability during heat stress.

A) Quantification of the average number of live pollen grains per flower +/- SEM in each genotype immediately upon harvesting. Three independent replicates were quantified with each replicate containing 4 flowers per genotype. B) Representative confocal micrographs of pollen grains of VF36, *are*, *are* complemented with a *35S-F3H* transgene (*are*-T5), and VF36 transformed with this same transgene (VF36-T3). Pollen grains incubated at either 28°C or 34°C for 2 hrs and then co-stained with FDA (denoting live grains in green) and PI (denoting dead grains in magenta). Scale Bar: 50 µm. C) Quantification of the percentage of viable grains of VF36, *are*, *are*-T5, and VF36-T3 after 2 hr incubation at 28°C or 34°C from four independent experiments is reported with each replicate containing 3 flowers per genotype. Asterisks denote significant differences from VF36 at the same temperature and hash marks denote significant differences between temperatures within the same genotype according to a two-way ANOVA followed by a Tukey post hoc test with a $p<0.05$.

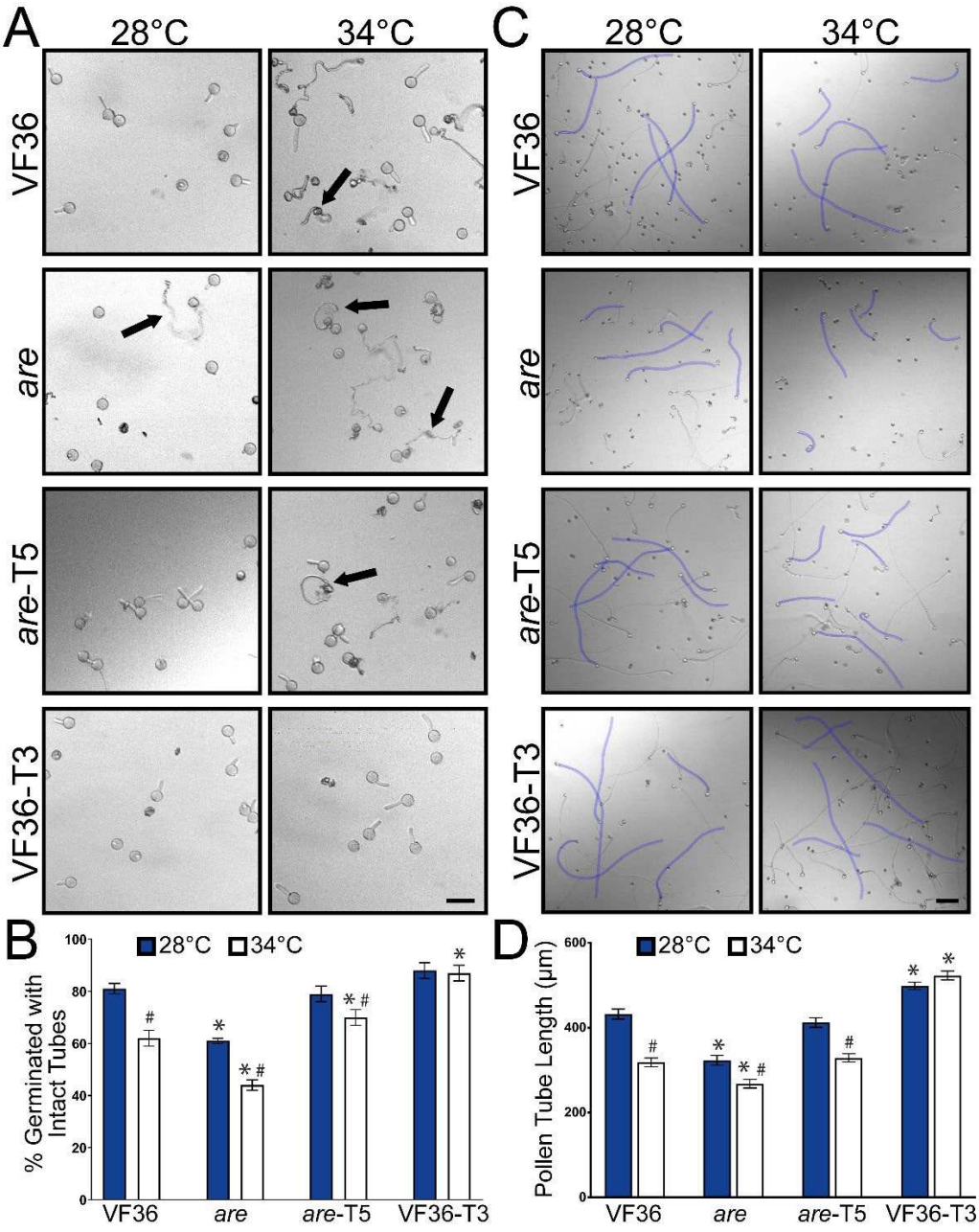

Figure 3. The negative effects of high temperature on tomato pollen germination and tube length are accentuated in *are* and reversed by an *F3H* transgene.

A) Representative brightfield images of VF36, *are*, are *are-F3H*-T5, and VF36-*F3H*-T3 pollen germination after 30 min at either 28°C or 34°C. Arrows denote ruptured pollen. Scale bar: 50 µm B) Quantification of percent pollen germination that exhibited intact tubes after 30 min. C) Representative images of pollen tubes elongating for 120 min at 28°C, or at 30 min at 28 °C then transferred to 34°C for an additional 90 min. Five pollen tubes from each image are highlighted in blue to enhance visibility. Scale bar: 100 µm. D) Quantification of mean pollen tube length is shown. Error bars represent standard error of the mean. Asterisks denote significant differences from VF36 at the corresponding temperature and hash marks denote significant differences between temperatures within the same genotype according to a two-way ANOVA followed by a Tukey post hoc test with a $p<0.05$ ($n> 90$ grains or 200 pollen tubes per genotype and treatment).

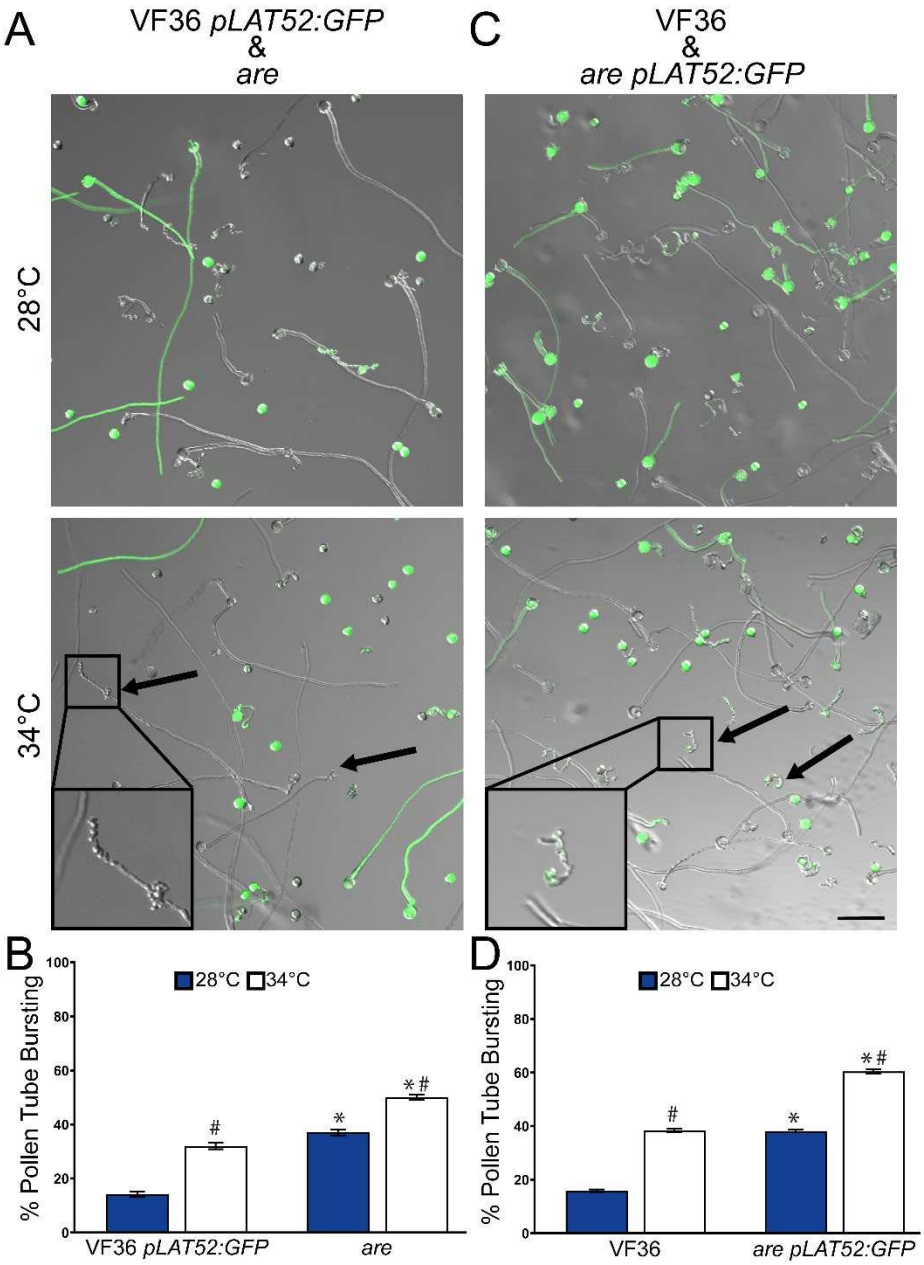

Figure 4. The heat accentuated rupturing of *are* pollen tubes is not improved by culturing with the parental line.

A) Representative images of pollen tubes of VF36 *pLAT52:GFP* (green) germinated along with untransformed *are*. Pollen was germinated *in vitro* and for 120 min at 28°C or for 30 min at 28°C followed by 90 min at 34°C. B) Quantification of mean percent pollen tube rupture for VF36 *pLAT52:GFP* and *are* (n> 500 pollen grains for each genotype from 3 biological replicates with 6 technical replicates within each sample). Error bars represent standard error of the mean. C) Representative images of pollen tubes of VF36 germinated with *are pLAT52:GFP* (green). D) Mean percent pollen tube rupture ± SEM for VF36 and *are pLAT52:GFP* (n> 500 pollen grains for each genotype from 3 biological replicates with 6 technical replicates within each sample). Scale bar: 100 µm. Arrows denote ruptured pollen in *are*.

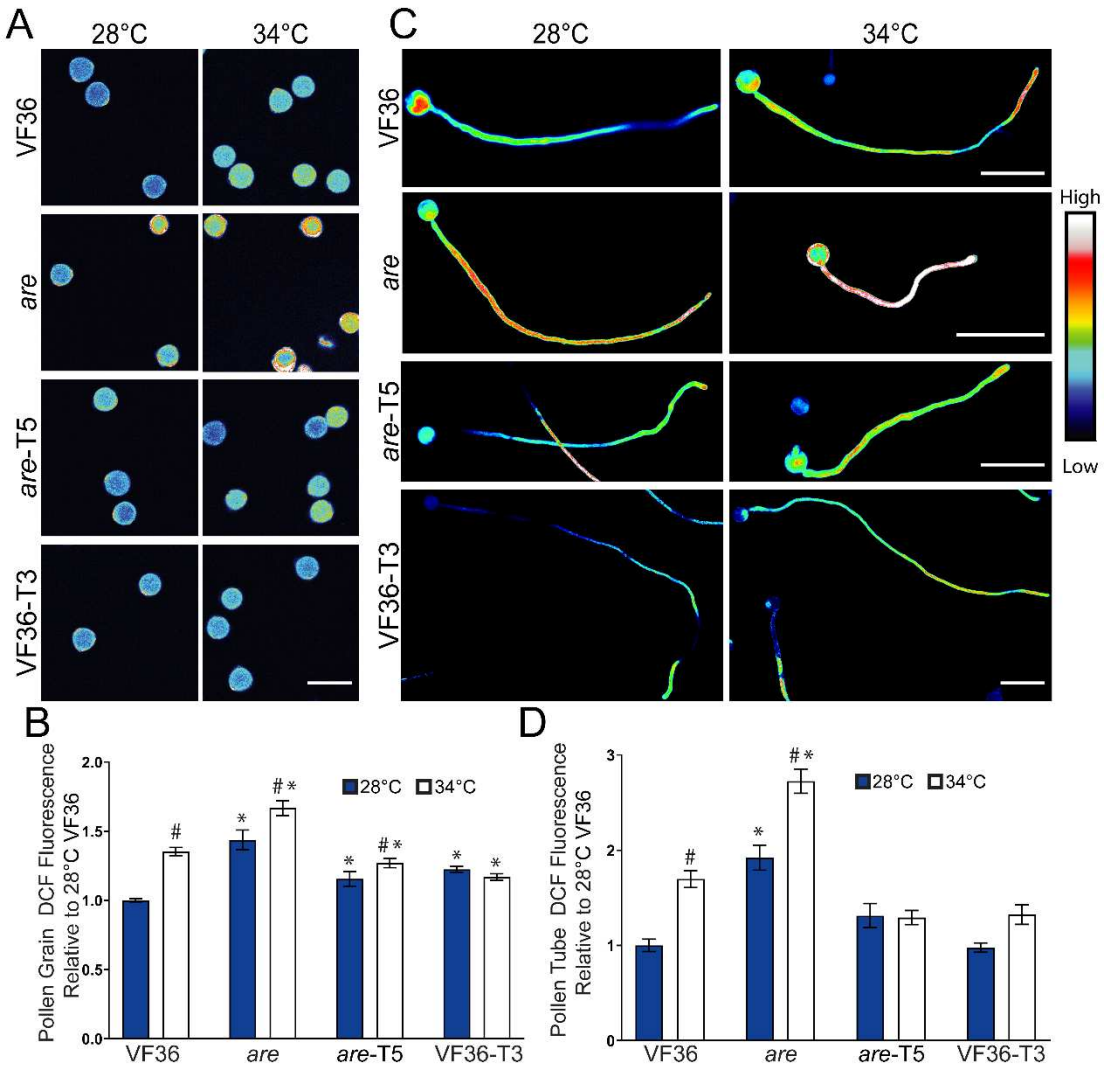

Figure 5. Heat-induced ROS accumulation in germinating pollen grains and elongating pollen tubes is reduced with increased flavonol synthesis.

A) Representative confocal micrographs of pollen grains germinated for 10 minutes and then stained with CM-H_2DCFDA for 20 mins. DCF fluorescence has been converted to a LUT scale for visualization. Scale Bar: 50 µm. B) The mean fluorescence of germinating pollen relative to VF36 at 28°C across 4-5 independent experiments is reported with the error bars representing the standard error of the mean (n> 89 grains per genotype and treatment). C) Representative fluorescent images of pollen tubes germinated for 30 mins at 28°C, and then transferred to 28°C or 34°C for an additional 90 min. Pollen tubes were then stained with CM-H_2DCFDA for 20 mins. DCF fluorescence has been converted to a LUT scale for visualization. The VF36-T3 images are zoomed out as these pollen tubes are longer. Scale Bars: 100 µm. D) The mean fluorescence of elongating pollen tubes relative to VF36 at 28°C across 3 independent experiments is reported with the error bars representing the standard error of the mean (n> 85 tubes per genotype and treatment). Fluorescence values were normalized to the VF36 pollen germinated at 28°C. Asterisks denote significant differences from VF36 at the same temperature and hash marks denote significant differences between temperatures within the same genotype according to a two-way ANOVA followed by a Tukey post hoc test with a $p<0.05$.

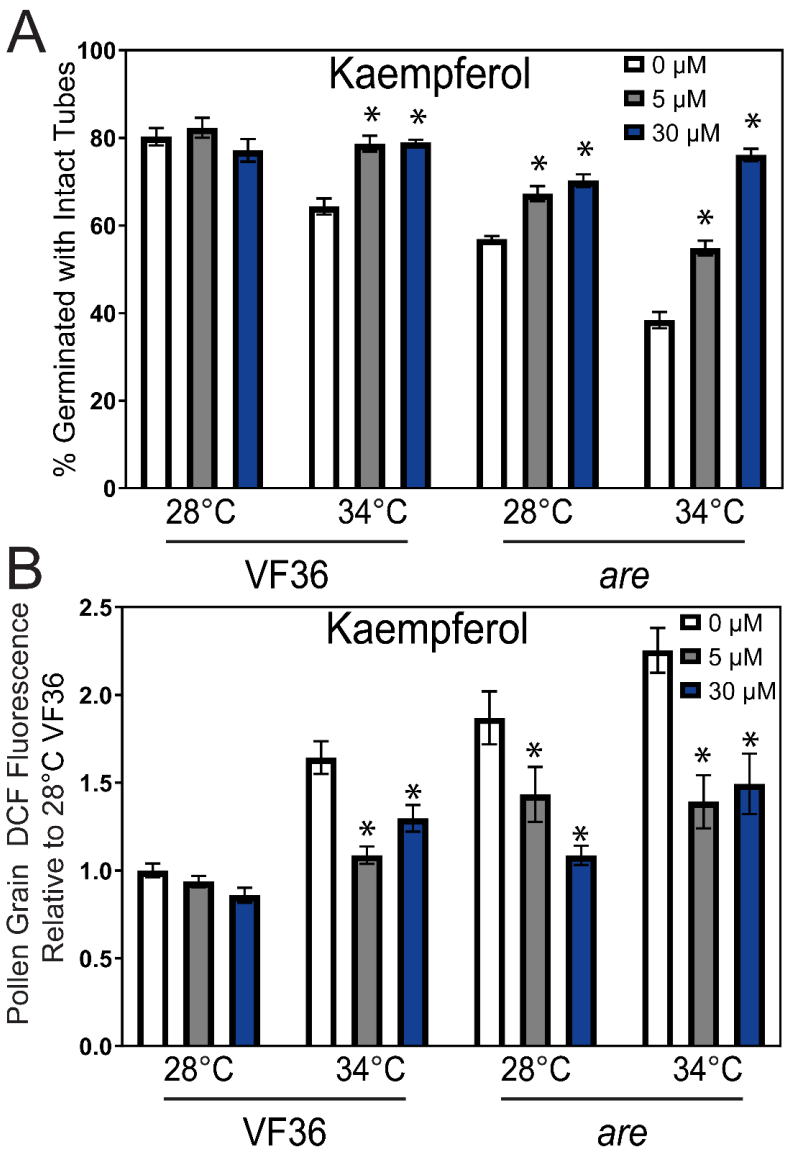

Figure 6. Impaired pollen germination in *are* is reversed by supplementation with the flavonol, kaempferol.

A) Percent pollen germination of VF36 and *are* after exogenous kaempferol treatment at doses of 0, 5, or 30 µM at 28°C or 34°C. The effect of these three flavonols on percent germination was determined in 3-4 independent experiments with n> 80 grains. B) The mean DCF intensity of germinating pollen grains incubated with 0, 5, or 30 µM kaempferol relative to VF36 at 28°C across 4 independent experiments is reported (n> 40 grains per genotype and treatment) Error bars represent standard error of the mean. Asterisks denote significant differences from 0 µM flavonol treatment within that genotype and temperature treatment according to a two-way ANOVA followed by a Tukey post hoc test with a $p<0.05$.

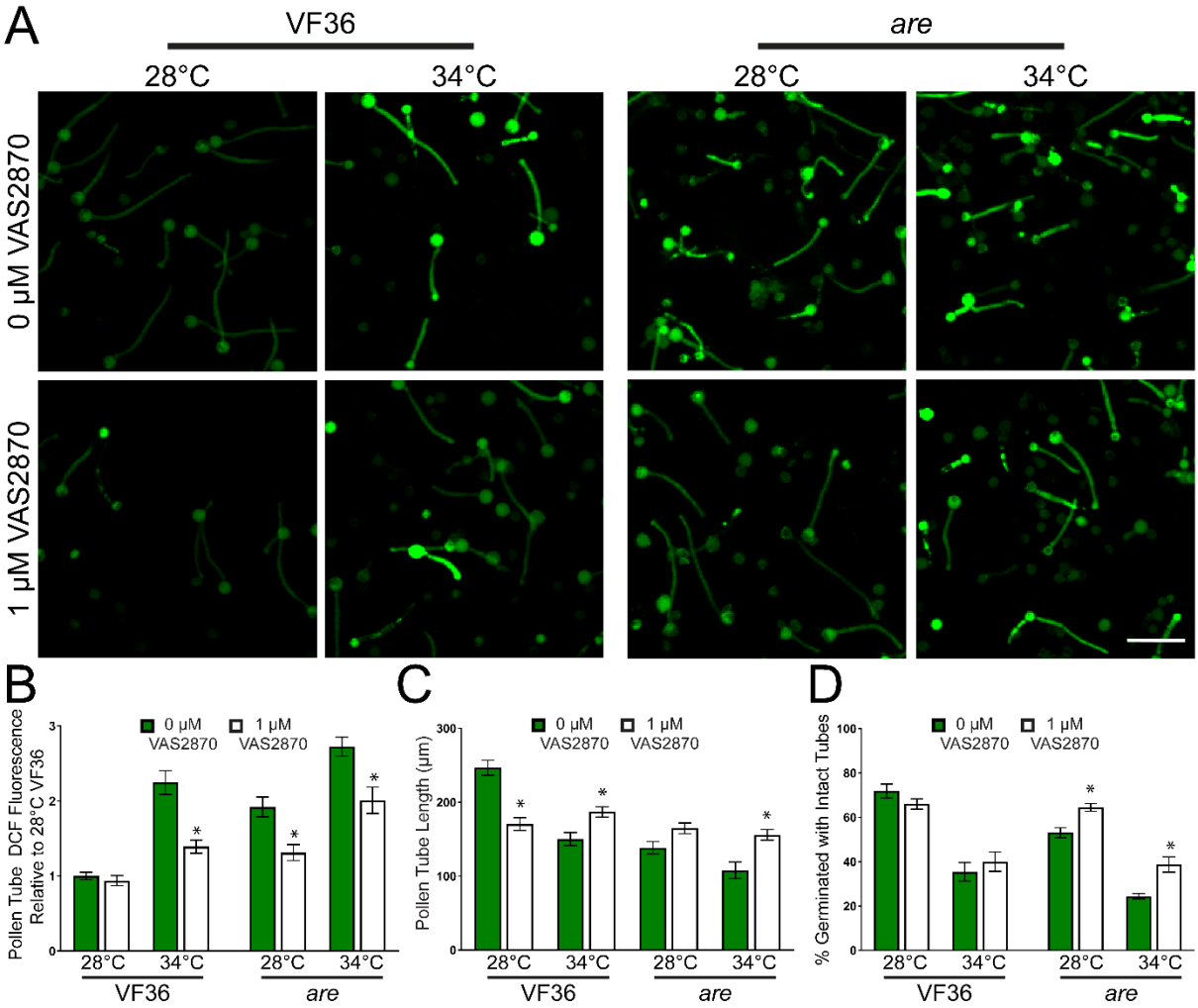

Figure 7. Inhibition of RBOH activity reduces heat induced ROS accumulation and impaired pollen performance.

A) Representative confocal micrographs of DCF fluorescence intensity of elongating pollen tubes treated with 1 µM of the pan-RBOH inhibitor VAS2870. Quantification of average and SEM of B) DCF fluorescence intensity, C) pollen tube length and D) germination in PGM containing VAS2870 across 4 independent experiments is reported (n> 200 grains or 62 tubes per genotype and treatment). Pollen was incubated at 28°C or 34°C. Asterisks denote significant differences from 0 µM VAS2870 treatment within a particular genotype and temperature treatment according to two-way ANOVA followed by a Tukey post hoc test with a $p < 0.05$.

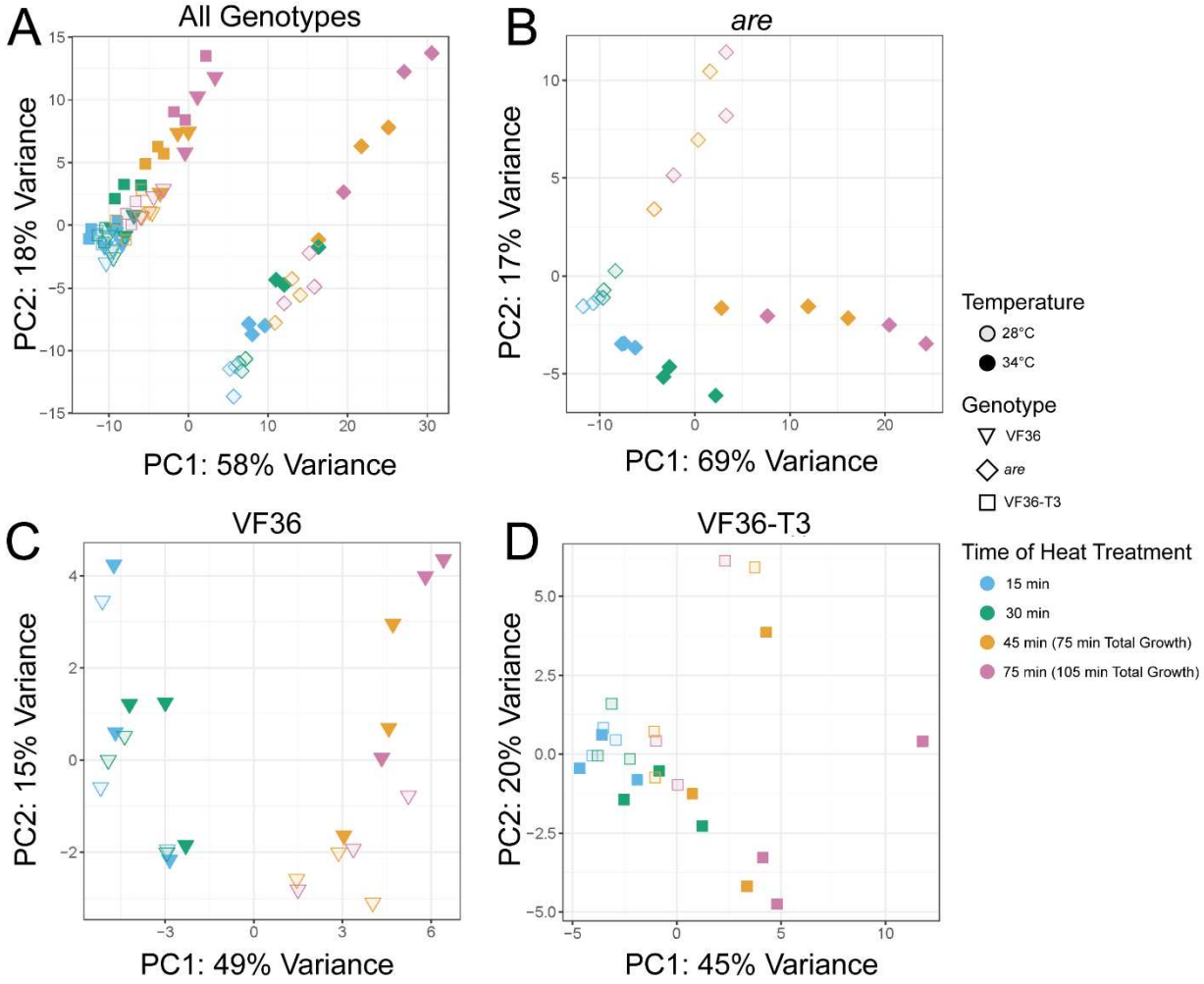

Figure 8. PCA plots highlight distinct transcriptional responses between *are* and the other two genotypes and in response to elevated temperature.

A) PCA plot for all samples analyzed via RNA seq. The samples in the right cluster are all *are* samples, while the group on the left contains both VF36 and the VF36-T3 samples. Individual PCA plots for each genotype reveal the time and temperature response within each genotype with B) *are* C) VF36 and D) VF36-T3 samples.

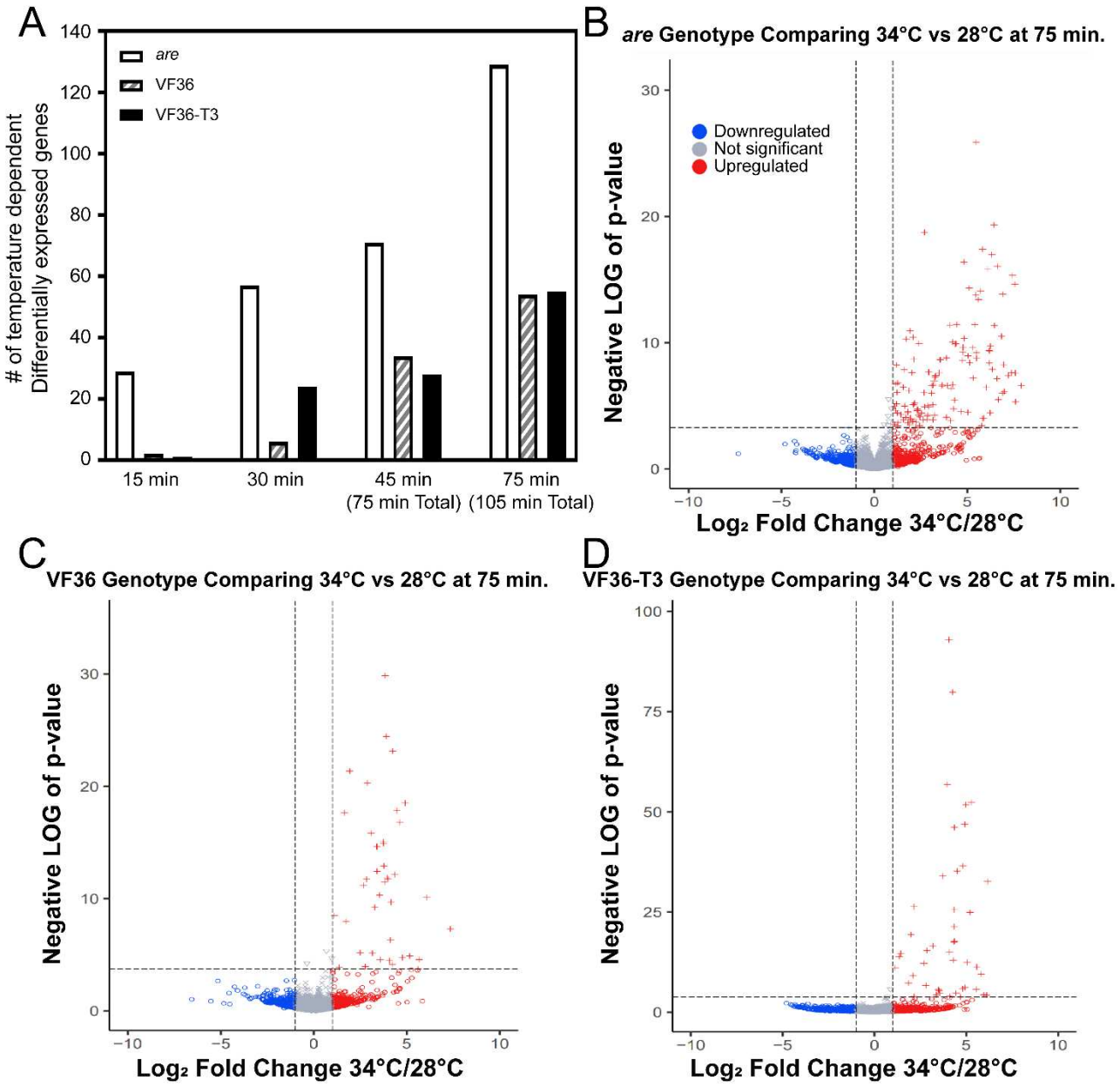

Figure 9. Transcriptional responses increase across the duration of temperature stress and are accentuated in the *are* mutant.

A) The number of differentially expressed (DE) genes at 34°C relative to 28°C within each genotype as determined using EdgeR are graphed as a function of time of pollen tube growth for VF36, *are*, and VF36-*F3H*-T3. These genes were defined as DE if they had an Adjusted *P*-value <0.05 and log fold change greater than or less than 1. B-D) Volcano plots of the log fold change at 34° C relative to 28°C and p-values for all samples. The dotted lines represent P-value cut-offs of 0.05 and Log_2 fold change of 1. B) *are*, C) VF36 and D) VF36-*F3H*-T3. Blue circles denote genes that are down-regulated (Log_2 fold change below 1), red crosses indicate genes that are upregulated (Log_2 fold change above 1), while gray circles denote genes that do not display a Log_2 fold change above or below the cutoff of 1.

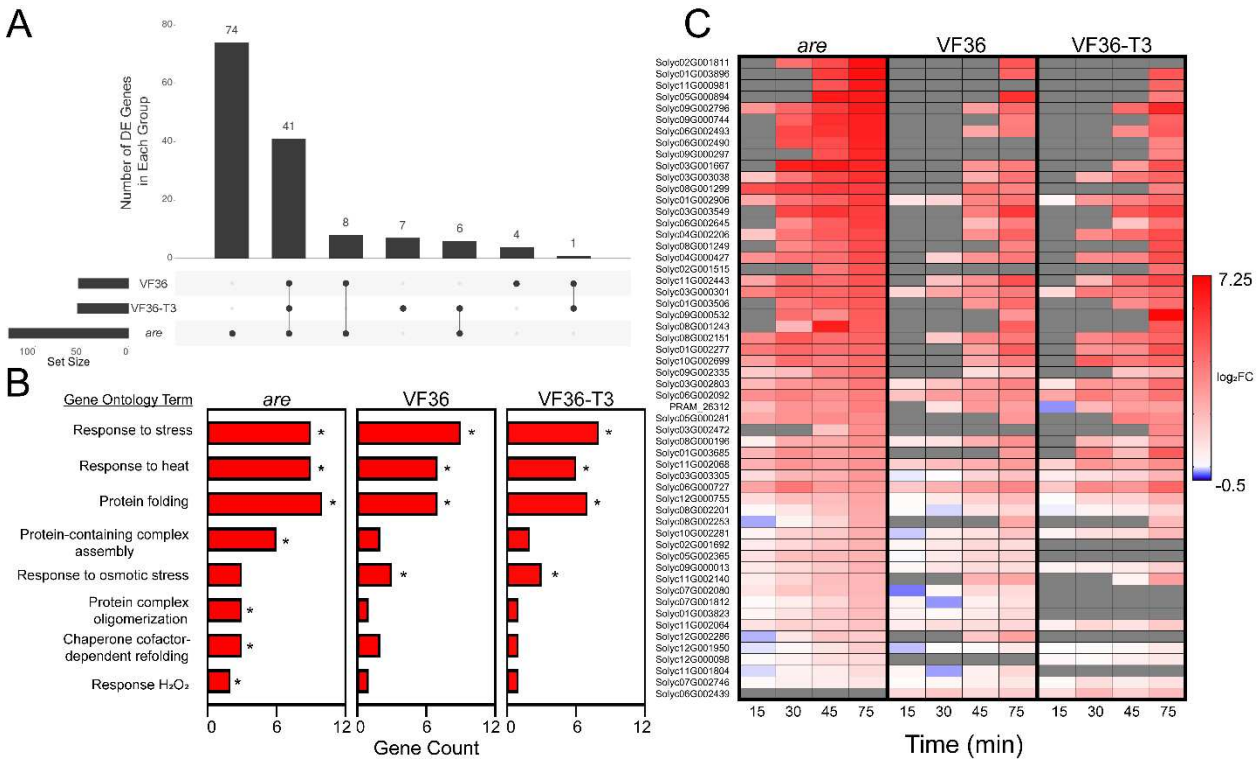

Figure 10. The heat-dependent transcriptional response of *are* occurs more rapidly and contains a greater number of unique transcripts.

A) Upset plot of temperature-dependent differentially expressed (DE) genes within each genotype after 75 min heat treatment (105 minutes total growth). Numbers above bars represent the number of temperatures regulated DE genes that are shared between genotypes connected by lines. Set size refers to the number of DE genes at this specific timepoint for each genotype. B) Biological processes that are significantly enriched in transcripts that are DE at the elevated temperature in the *are* mutant were determined using String. Groups that were significantly enriched in the *are* mutant are reported. The number of genes in each group were determined for the other genotypes. * Indicates the groups for which enrichment was significant relative to genome. C) Heatmap of the 56 genes that were found to be DE in two or more genotypes after 75 min heat treatment (105 minutes total growth) as shown on the Upset plot). The temperature-dependent log2 Fold Change (log2FC) of these genes was then mapped back to pollen samples taken at the earlier timepoints. Genes are ranked by highest logFC in *are* at the 75 min timepoint (105 minutes total growth). Gray boxes represent no detected expression at that timepoint. All genes IDs utilized in all figures refer to the SL5 version of the tomato genome (Zhou et al., 2022).

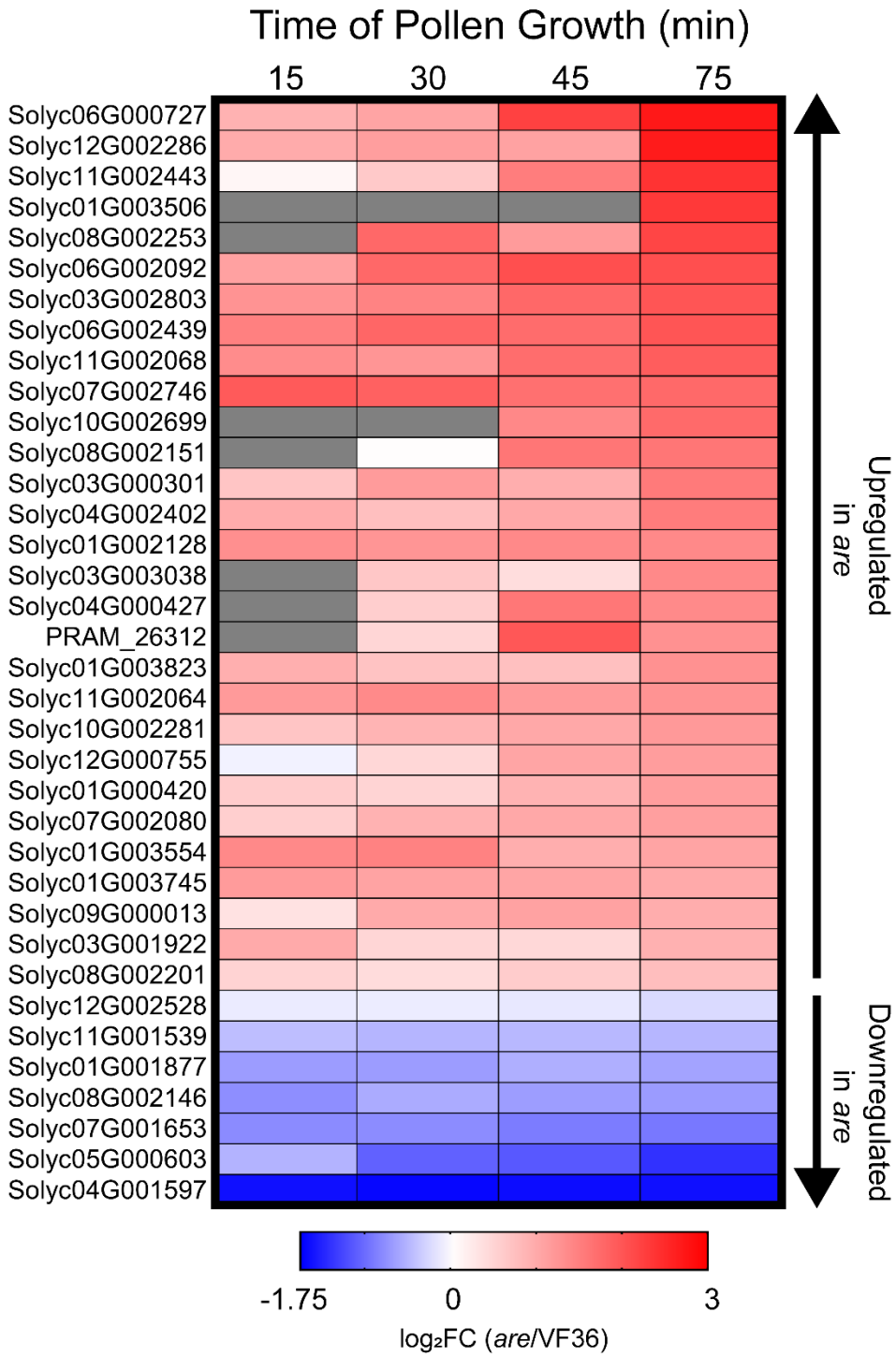

Figure 11. *are* displays an upregulated heat response even at optimal temperatures.

A) Heatmap of the 36 genes encoding heat shock factors that were found between *are* and VF36 at 28°C. log2 Fold Change (log2FC) of *are* relative to VF36 for these genes was then mapped back to pollen samples taken at the earlier timepoints. Genes are ranked by highest logFC in *are* at the 75 min timepoint (105 minutes total growth). Gray boxes represent no detected expression at that timepoint.